Research Square

Preprints are preliminary reports that have not undergone peer review.
They should not be considered conclusive, used to inform clinical practice,
or referenced by the media as validated information.

A Machine Vision–Based Method for Quantitative Spray Pattern Analysis and Nozzle Optimization in Precision Weed Sprayers

Vinay Vijayakumar
University of Florida, IFAS
Yiannis Ampatzidis
i.ampatzidis@ufl.edu

University of Florida, IFAS
Antonio de Oliveira Costa Neto
University of Florida, IFAS
Tom Burks
University of Florida
Won Suk Lee
University of Florida
John Schueller
University of Florida

Research Article

Keywords: image processing, precision agriculture, smart sprayers, vegetables

Posted Date: May 21st, 2026

DOI: https://doi.org/10.21203/rs.3.rs-9419383/v1

License: This work is licensed under a Creative Commons Attribution 4.0 International License.
Read Full License

Additional Declarations: No competing interests reported.

A Machine Vision–Based Method for Quantitative Spray Pattern Analysis and Nozzle Optimization in Precision Weed Sprayers

Vinay Vijayakumar[1,2], Yiannis Ampatzidis[1,2*], Antonio de Oliveira Costa Neto[1], Tom Burks[2], Won Suk Lee[2], John Schueller[3]

[1] Southwest Florida Research and Education Center, University of Florida, IFAS, 2685 SR 29 North, Immokalee, FL 34142, USA.
[2] Department of Agricultural and Biological Engineering, University of Florida, Gainesville, FL 32611, USA.
[3] Department of Mechanical & Aerospace Engineering, University of Florida, Gainesville, FL 32611, USA
* Corresponding author: i.ampatzidis@ufl.edu

Abstract

Precision weed sprayers require optimized nozzle selection and operating conditions to minimize spray dispersion and drift while ensuring effective target coverage. However, existing studies primarily focus on conventional high-volume sprayers, droplet-level analyses, or aerial applications, leaving a gap in methods tailored to ground-based robotic precision sprayers operating under dynamic conditions. In addition, nozzle manufacturers provide limited information beyond spray angle and flow rate, lacking practical guidance on spray coverage under varying heights, motion, and wind. This study introduces a low-cost, machine-vision-based methodology for quantitative evaluation of spray patterns and systematic nozzle selection for robotic precision weed sprayers. The proposed framework integrates simple experimental setups with image-based analysis to extract key spray metrics, including spray area, width, and length, under varying operational conditions. Experiments were conducted on a robotic sprayer platform using even flat-fan nozzles (15° and 25°) under static and dynamic conditions, including different pressures, spray heights, vehicle speeds, and simulated wind. Statistical analyses were performed to quantify the effects of these factors on spray characteristics. Results identified optimal conditions for the 15° nozzle at 103.42–137.89 kPa and 63.5 cm spray height, achieving reduced spray area and improved drift resistance at vehicle speeds below 0.89 m s^{-1}. The proposed method provides a practical and scalable approach for evaluating spray performance and selecting nozzle–operation combinations for precision applications. This work advances the design and optimization of robotic sprayers and supports more efficient and sustainable weed management practices.

Keywords: image processing, precision agriculture, smart sprayers, vegetables.

1. Introduction

Precision application of agrochemicals reduces the adverse effects of conventional sprayers by optimizing spray delivery, thereby minimizing wastage, crop damage, environmental pollution, and the overall cost of weed control (Chen et al., 2021; Ma et al., 2026; Vijayakumar et al., 2023). Although several alternative non-chemical weed control methods have been explored in specialty crops, including thermal approaches such as flame (Datta and Knezevic, 2013), steam (Abdulridha et al., 2019; Abdulridha et al., 2023), and laser (Rakhmatulin and Andreasen, 2020; Carbon Robotics, 2022), their adoption remains limited due to operational complexity, energy requirements, and scalability challenges (Barbosa Júnior et al., 2024). Consequently, chemical-based precision spraying remains the most

practical and widely adopted solution, highlighting the need to optimize sprayer performance to reduce off-target application and improve efficiency.

Optimization of spraying systems involves multiple interacting components, including control strategies, fluid delivery systems, and, critically, nozzle selection. Nozzles play a central role in determining spray distribution, coverage, and drift potential (Wolf and Bretthauer, 2009). Previous studies have primarily focused on nozzle performance under conventional spraying scenarios, often assuming constant application rates (e.g., 141 L ha^{-1}) and steady operating conditions (Meyer et al., 2016). Other studies have emphasized droplet size characterization using advanced instrumentation such as Phase Doppler Particle Analyzers (PDPA) to support drift modeling (Nuyttens et al., 2011). While valuable, these approaches are often impractical for precision spraying systems, where multiple factors, including spray height, intermittent actuation, vehicle motion, and environmental disturbances, interact dynamically and cannot be adequately captured through droplet-level measurements alone.

Existing nozzle selection guidelines are largely designed for conventional broadcast sprayers and focus on parameters such as nozzle spacing, overlap, and spray angle (Wolf and Bretthauer, 2009; Johnson and Swetnam, 1996; Grisso et al., 2019). These guidelines do not address the unique operational characteristics of precision sprayers, particularly robotic and spot-spraying systems that operate at lower application volumes, variable speeds, and intermittent spraying conditions. Similarly, studies on aerial spraying systems provide insights into drift potential (Hunter et al., 2020; Liu et al., 2026), but their findings are not directly transferable to ground-based platforms due to differences in airflow dynamics, application geometry, and target proximity.

Several efforts have been made to evaluate precision spraying systems; however, important limitations remain. Baltazar et al. (2021) assessed a robotic sprayer using water-sensitive papers, focusing on droplet size and coverage for canopy applications, but did not analyze spray drift or spatial spray distribution. Hussain et al. (2020) evaluated spray targeting using water-sensitive papers and image-based blue ratio metrics; however, their approach did not quantify spray displacement or provide a detailed characterization of spray area per nozzle. Other studies have focused on system-level benefits such as herbicide savings (Spaeth et al., 2024), rather than fundamental spray behavior. Moreover, although several AI-enabled smart sprayers have been developed (Partel et al., 2019; Partel et al., 2021; Ruigrok et al., 2020; Vijayakumar et al., 2026), there is still a lack of quantitative, scalable, and practical methods to evaluate spray patterns and drift under realistic operating conditions.

A critical gap, therefore, exists in the availability of simple, low-cost, and quantitative methodologies for evaluating spray patterns and guiding nozzle selection specifically for robotic precision sprayers. Such systems require evaluation approaches that go beyond traditional droplet analysis and instead capture spatial spray characteristics under both static and dynamic conditions. In particular, there is a need to quantify how spray area, shape, and displacement vary with operational parameters such as pressure, nozzle type, spray height, vehicle speed, and wind, and to translate this information into actionable guidelines for system design and optimization.

To address this gap, this study proposes a novel machine-vision-based framework for spray pattern evaluation and nozzle selection tailored to robotic precision weed sprayers. The primary contribution of this work is the development of a practical, low-cost, and scalable methodology that combines controlled experiments with image-based analysis to quantify key spray characteristics, including spray area, width, length, and drift behavior. Unlike prior approaches, the proposed method evaluates spray performance under both static and dynamic conditions, including simulated wind and moving platform scenarios, thereby capturing realistic field operating conditions.

The methodology was implemented on a robotic smart sprayer platform and applied to evaluate two even flat-fan nozzle types (15° and 25°) across a range of pressures, spray heights, and vehicle speeds as a case study. The resulting dataset enabled a systematic analysis of the relationships between operational parameters and spray behavior, leading to the identification of optimal nozzle configurations and operating conditions. Ultimately, this work provides a generalizable framework for spray evaluation

and nozzle selection, contributing to improved design, calibration, and deployment of precision spraying systems for sustainable weed management.

The remainder of this paper presents the nozzle selection framework, followed by detailed descriptions of the experimental setup and testing procedures, including static tests (with and without wind) and dynamic tests conducted on the robotic platform. Results and discussion focus on the quantitative analysis of spray characteristics and the identification of optimal operating conditions for precision weed spraying applications.

2. Materials and Methods

2.1 Robotic smart sprayer platform

In this study, a robotic smart sprayer platform (Figure 1) was utilized as a case study, with a frame built from aluminum extrusions (40 mm x 40 mm), which includes two motorized 14" (35.56 mm) diameter wheels (24 V DC, 200 W) driven by two 12 V batteries (Eco-worthy, California, USA). A smaller test frame constructed from 1" square aluminum tubes was used to mount the nozzles and the camera for capturing the spray pattern. Four pumps, two Vevor pumps (Houston, Texas, USA; 12V DC, 20.82 LPM and two Seaflo 55 Series pumps (Indiana, USA; 12V DC, 5.5 GPM) were used for the spraying system. The robotic smart sprayer was built to target three types of weeds (broad leaf, sedge, and grass leaf) on vegetable (pepper and tomato) plasticulture beds (Vijayakumar et al., 2025).

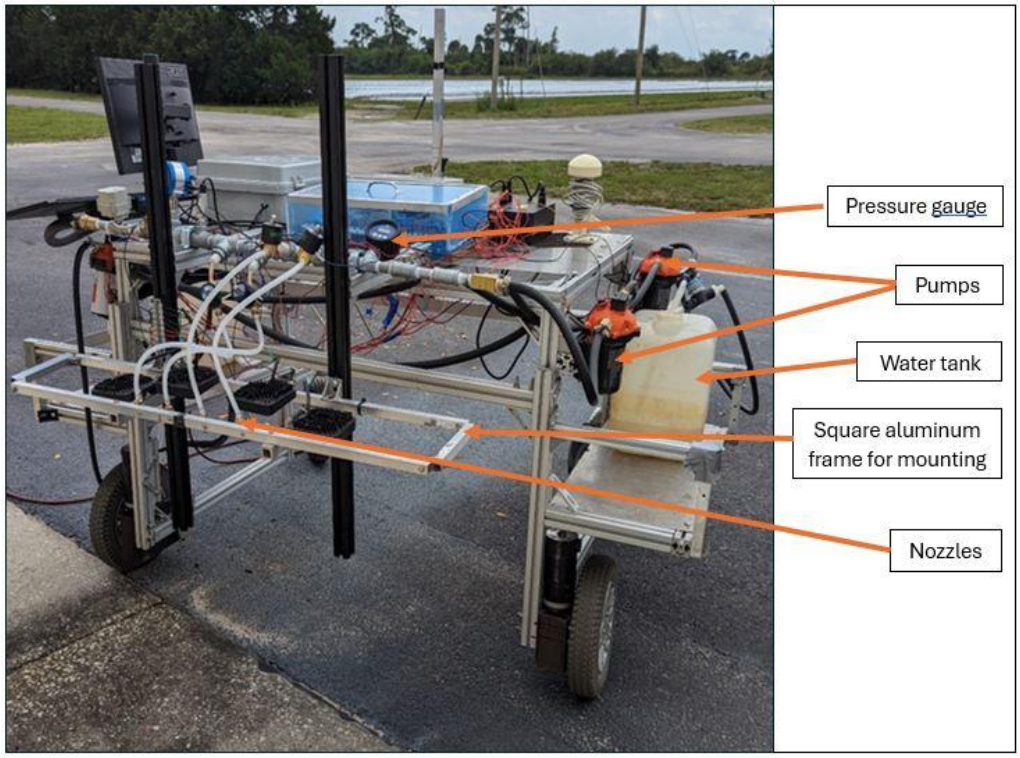


Figure 1. Robotic smart sprayer platform utilized in this study.

2.2 Nozzle selection process

Choosing the right nozzles is an important part of designing a precision spraying system. The nozzle type chosen would determine the spray coverage, spray volume, droplet characteristics, spray drift, and the required operating pressure for applying herbicides (Johnson & Swetnam, 1996; Hofman & Solseng, 2004). Multiple factors influence the decision-making steps for nozzle selection; some of them are:

a) **Weed type**

The type of weeds and the intended time of application of the spray influence the nozzle selection process. This dependency is due to the varying droplet sizes affecting the weed coverage. Coarse droplets tend not to stick to grass leaf weeds and certain broadleaf weeds such as lambsquarters (Wolf, 2011). Early-stage weeds might also require medium to small droplets to prevent the spray from missing smaller weed targets with cotyledons or smaller leaves. In general, the size of the plants and the leaves also influence nozzle selection (Wolf, 2011).

b) **Pressure**

The operating pressure affects the nozzle flow rate, droplet size, and the spray angle of the nozzle (Wolf, 2011). Nozzle manufacturers specify the minimum pressure for the nozzles, which refers to the lowest operating pressure of the nozzle. The target pressure is usually the mid-point between maximum and minimum pressures, which should ideally give an optimal spray pattern and spray coverage. The spray droplet gets coarser as the nominal flow rate increases at lower pressures (Wolf, 2011).

c) **Travel speeds**

For broadcast herbicide spraying at slower travel speeds, experts recommend forward oriented nozzles. A downward pointing nozzle orientation is recommended for better spray penetration in denser canopies (Wolf, 2011). In this study, the selected nozzles point downwards with zero angle to reduce the distance the spray droplets must travel from the nozzle to the target weed and to prevent any residual drift due to gravity that might come into play if the nozzle is at an angle. Canopy penetration improves with slower travel speeds and higher carrier volumes for all types of nozzles. Lower travel speeds generally result in better coverage because of lower drift (Wolf, 2011).

d) **Droplet characteristics**

Nozzles come in different types that can generate droplets of varying sizes: very fine, fine, medium, coarse, and very coarse droplets (Wolf and Bretthaue, 2009). These droplets have varying behavior in canopy penetration and response to drift. As the pressure is increased, nozzles produce finer droplets. It is recommended to avoid fine spray nozzles to avoid drift (Wolf, 2011).

Nozzles commonly used in spraying applications are available in different types, such as flat-fan nozzles, flood nozzles, hollow-cone nozzles, raindrop nozzles, full-cone nozzles, etc. (Johnson & Swetnam, 1996). They produce a variety of spray patterns. Each of these nozzles has its advantages and disadvantages, as described in Table 1.

Table 1. Example of different standard nozzle types and their characteristics.

Nozzle Type	Pressure range (kPa)	Advantages	Disadvantages
Standard flat-fan	206.84-413.68; 206.84-275.79 (ideal range) (Grisso et al., 2019)	Allows lowest water volumes; Reliable performance	Cannot use higher pressures; drift prone (Hofman and Solseng, 2004)
Even flat-fan	137.89-206.84 (Summer, P., E., 2012)	Provide uniform coverage across the entire width of the spray pattern (Grisso et al., 2019).	Controlling the release height and spray angle provides control over

			spray bandwidth (Grisso et al., 2019)
Extended range flat-fan	103.42-413.68	Good drift control; provides great spray distribution over wide pressure ranges; works well on sprayers equipped with flow controllers (Grisso et al., 2019)	------
Flood nozzles	68.95-172.40	Good for suspension fertilizers where clogging is a potential problem; produces large droplets.	Not suited for contact herbicides and requires 100% overlap (Johnson and Swetnam, 1996).
Raindrop nozzles	137.89-344.74	Large drops in a hollow cone pattern Good for herbicide incorporation (Johnson and Swetnam, 1996).	Requires 100% overlap to ensure uniform coverage; not suitable for post-emergence herbicides (Johnson and Swetnam, 1996).
Hollow cone	40-100	Good for applications needing foliage penetration and complete coverage of the leaf surface (Johnson and Swetnam, 1996).	Smaller droplets mean higher drift potential (Grisso et al., 2019).
Full cone	15-40	Drift resistant because of larger droplets; works well with sprayers equipped with flow controllers (Johnson and Swetnam, 1996).	Higher percentage overlap might be required (100%) (Grisso et al., 2019).

Considering the target application (i.e. either broadcast spraying or uniform spraying, type of sprayer system for example ground-based or aerial) is essential when choosing a nozzle. In this study, the nozzles were selected for a precision spraying application using a robotic smart sprayer platform and not for a broadcast or uniform spraying application. Consequently, the recommendations provided by many nozzle experts, who suggest specific parameters such as optimum overlap, drift resistance, and uniform coverage, which are effective for broadcast spraying applications, proved unsuitable for precision spraying applications. This is because precision spraying involves nozzles that operate for shorter durations and potentially at lower pressures.

Hence, based on the final application requirements, the nozzle selection considerations, and recommendations provided in the previous section, a plan was established to determine the decision-making steps to select the available options for the initial procurement of nozzles and then perform a series of tests on the nozzles to experimentally determine the best option for the robotic smart sprayer platform. The decision-making steps employed for the initial procurement of nozzles can be categorized as:

1 Weed-dependent decision: Since the early-stage application is targeted when the weeds are smaller, this eliminates the nozzles that produce “very fine” and “fine” droplets. However, highly coarse droplets do not perform well on grassy weeds and some broad leaf weeds (Wolf, 2011). Hence, medium droplets might be better suited for this application.

2 Pressure range: A pressure that can be achieved by a direct current (DC) motor while also being good enough to provide enough spray strength to prevent drift is the ideal option. Consequently, nozzles within a pressure range of 68.95 kPa – 689.5 kPa (10 Psi – 80 Psi) were better options for the smart spraying system.

3 Pan angle: As smaller weeds are targeted at an early stage, narrow cone angle nozzles (15°, 25°, etc.) were preferred since they achieve a smaller spray area (bandwidth and/or total area).

4 Operation and performance at different boom heights: For the smart spraying system, a nozzle that can provide a steady spray at lower pressures, at different boom heights between 45.7 cm and 101.6 cm (18 inches – 40 inches) is required. This takes into consideration the plant height (7.62 cm - 25.4 cm), bed height (20.32 cm - 30.48 cm), and an additional buffer space (12.90 cm - 38.71 cm) for the nozzles to spray. The nozzles on the robotic smart spraying system should be closer to the plants to provide a uniform drift-resistant spray.

5 Travel speeds: The operating speed of the robotic smart sprayer platform is a crucial parameter in determining the nozzle type. Through multiple tests, it was determined that the typical operating speed for good target (i.e., types of weeds and crops) detection by a computer vision system is 1 m/s – 1.34 m/s. Beyond this speed, the performance of the AI-enabled detection model in real time is reduced significantly because of image blurring. Hence, it is essential to test the drift resistance of the nozzles for these speeds.

6 Performance under flow control methods: The selected nozzles should respond well to flow control methods such as proportional integral (PI), pulse width modulation (PWM), etc., and maintain spray quality for shorter and longer periods of spray, if needed.

7 Nozzle material: The right material is necessary to avoid corrosion because of exposure to water and chemicals. Stainless steel provides the right balance in terms of resistance to chemicals over a longer period, corrosion due to environmental factors, and price.

Based on these decision-making steps, the following two Veejet (Spraying Systems Co., Illinois, USA) nozzle types were initially selected for evaluation in this study:

1. The H1/4VV-SS1507 VeeJet Nozzle: Type: flat-fan nozzle; Material: 303 stainless steel. It has a rated spraying angle of 15° achieved at a pressure of 275.79 kPa. This nozzle would be referred to as the 15° nozzle henceforth in this study.
2. The H1/4U-SS2510 VeeJet Nozzle: Type: flat-fan nozzle; Material: 303 stainless steel. It has a rated spraying angle of 25° achieved at a pressure of 275.79 kPa. This nozzle would be referred to as the 25° nozzle henceforth in this study.

A preliminary analysis was necessary to narrow down the type of nozzle, the right spray height, the optimum pressure, the total number of nozzles required, the spacing between nozzles, and the right speed of operation. The 15° and 25° nozzles are the smallest available narrow-angle nozzles in the nozzle catalog of Veejet nozzles for spraying purposes, and two of each were selected for the preliminary analysis. The spray angle varies with pressure for each of these nozzles. Supplementary Table S1 summarizes the technical specifications of the nozzles.

The 15° and 25° nozzles are standard flat-fan nozzles with a tapered-edge spray pattern. The manufacturer (Spraying Systems Co.) provided a datasheet of the nozzles showing that the spray angle for both nozzles varies with the applied pressure (Supplementary Figure S1). The variation of flow rate for each nozzle is also shown in Supplementary Figure S1a. Even under some air velocity, medium droplets (236 – 340 micron volume mean diameter (VMD)) work well for narrow leaves, stems, and vertical leaves (such as grass leaf weeds), while coarse droplets (341 – 403 VMD) are great for broadleaf weeds with more flat leaf surfaces (Grisso et al., 2019). Choosing the 15° and 25° nozzles with different spray sizes that vary between fine to coarse spray provides us with options to test the characteristics of the spray at different pressures on a flat surface and on different weed varieties that respond differently to droplet sizes.

Supplementary Figure S1b shows the product performance chart for the 15° and 25° nozzles. One of the advantages of these nozzles is the ability to control the liquid flow rate and spray angle based on pressure. A pressure can be selected that offers the right balance between the right flow rate and drift resistance due to wind and/or the motion of the robotic smart sprayer platform. However, determining the right operating pressure for the nozzles requires testing the nozzle spray under static and dynamic conditions.

2.3 Testing method for nozzle selection

The deployment of a robotic smart sprayer platform in vegetable fields for real-time detection and targeted spraying of multiple weed species introduces significant operational challenges, particularly in the design and optimization of the spraying system. Key factors influencing performance include spray application height, drift susceptibility, platform travel speed, nozzle configuration, and required spray coverage per application event. Among these, nozzle selection plays a critical role, as it directly affects spray distribution, drift potential, and application accuracy.

Following the initial nozzle screening process (Section 2.2), two even flat-fan nozzle types were selected for further evaluation. However, rather than relying solely on manufacturer specifications or conventional selection charts, this study introduces a systematic experimental and machine-vision-based evaluation methodology to empirically determine optimal nozzle–operation combinations under realistic operating conditions. The proposed approach is designed to quantify spray behavior across varying spray heights, application pressures, and robotic platform speeds, enabling data-driven selection of operating parameters for precision spraying. The evaluation framework consisted of two complementary experimental components: **static tests** and **dynamic tests**, designed to capture spray behavior under controlled and field-representative conditions.

1. Static Tests: Static tests were conducted with the robotic sprayer platform in a fixed position to isolate the effects of pressure and spray height on spray pattern formation. These tests were further divided into two scenarios:

(a) No-wind (stationary) condition: The platform remained stationary in a controlled environment without airflow disturbances. Spray characteristics were captured using a machine-vision system, and key outputs included spray area and spray width. This setup provided baseline measurements of nozzle performance under idealized conditions.

(b) Simulated wind condition: To evaluate drift susceptibility, controlled airflow was introduced using a table fan to simulate wind effects. Under these conditions, both spray area and lateral spray displacement (spray shift) were quantified. This allowed assessment of nozzle stability and resistance to external disturbances.

2. Dynamic Tests: Dynamic tests were performed with the robotic platform moving at three representative operational speeds: 0.45 m s^{-1} (1 mph), 0.89 m s^{-1} (2 mph), and 1.34 m s^{-1} (3 mph). These speeds were selected based on the operational constraints of the machine vision-based weed detection system and represent realistic field deployment conditions. During motion, spray patterns were recorded and analyzed to quantify spray area and spray length under varying pressures. These experiments enabled the evaluation of spray distortion and drift behavior as a function of forward velocity, providing insights into nozzle performance under realistic, time-dependent operating conditions.

Proposed Methodological Contribution

The results from both static and dynamic experiments were integrated to establish a systematic, low-cost, and machine vision–driven framework for nozzle selection and spray system optimization. Unlike conventional approaches that rely on droplet characterization or manufacturer-reported parameters, the proposed method directly quantifies spatial spray behavior under controlled and operationally realistic conditions. This methodology enables the identification of an optimal operating window defined by spray height, pressure, nozzle type, and vehicle speed. Within this optimized range,

the spraying system is expected to achieve minimized spray footprint, improved targeting accuracy, and enhanced resistance to drift under both motion and wind disturbances.

It is important to note that the robotic platform and field configuration used in this study serve as a representative case study, demonstrating the applicability of the proposed framework. The methodology itself is generalizable and can be adapted to other robotic precision spraying systems and crop environments.

2.3.1. Static tests

a) Static test - Stationary (no wind) effect

Experimental setup

The robotic platform's spraying system was configured with four nozzles, two 15° nozzles and two 25°nozzles, linked to four solenoids (12V, 1.27 cm; US Solid, Ohio, USA). These solenoids, triggered by an Arduino MEGA (ELEGOO MEGA R3, China) through a 12V 4-channel relay (HiLetgo, Shenzen Hiletgo Technology Co., Limited, China), to control the nozzle activation. The nozzles were connected to the solenoids using 0.95 cm vinyl tubes and affixed to a 2.54 cm x 2.54 cm square aluminum tube (Figure 1).

The experiments were conducted at three different heights, 63.5 cm, 76.2 cm, and 101.6 cm above the ground. The lower height limit was set at 63.5 cm from the ground to ensure proximity to plants on the beds. The typical height of plants on the beds is approximately 33.02-50.8 cm (20.32-25.4 cm bed height and 12.7-25.4 cm plant height before reaching maturity). An additional 12.7 cm buffer was incorporated to prevent the nozzles from being too close to the plants, allowing sufficient space for the spray to be spread effectively. The maximum spray height was set at 88.9 cm during testing due to preliminary trials indicating that beyond this height, the distance between the nozzle and the target weeds would be too substantial, making it susceptible to drift.

Once the nozzles on the square frame (Figure 2a) were positioned at the appropriate height, the control system's pressure was adjusted across seven settings, ranging from 69.95 kPa to 275.79 kPa with 34.47 kPa increments. The selection of the lowest pressure point, 69.95 kPa, was determined by considering nozzle characteristics such as spray pattern, spray angle, and the minimum pressure required to effectively target weeds without resulting in a dripping spray application. Below 69.95 kPa, it became evident that the spray pressure was insufficient and not strong enough to withstand mild changes in wind speed, particularly at greater heights. Referring to the nozzle spray angle vs pressure curve (Supplementary Figure S1), it was noted that the nozzles achieve the rated pan angle at 275.79 kPa. This information guided the selection of the pressure range for the experiment, ensuring optimal performance while avoiding excessive pressure that could compromise the accuracy and effectiveness of weed targeting.

An 88.9 cm by 55.88 cm brown paper was placed underneath the nozzle to capture the spray patterns (Figure 2b). Brown paper sheets were used instead of water sensitive paper, as the most commonly available sizes of the water sensitive paper were smaller sizes (2.54 cm x 7.62 cm, 5.08 cm x 7.62 cm, 2.54 cm x 50.8 cm), which would not work for the nozzle sprays at higher pressure. The biggest available size of the water sensitive paper is 9.75”x11.75”, which might work for the sprays from the 15° nozzle, but would not work for the 25° nozzle at higher pressures. Furthermore, it might not be big enough to capture the shift in position during the wind test. The brown paper is also a significantly cheaper option that can absorb the sprays well and provides a large canvas to capture sprays in all types of experiments.

An Arduino code activated each 15° and 25° nozzle individually for a duration of 100 ms. This time duration is expected to be practical during field tests, considering the expected speeds of the robotic platform (ranging from 1 to 1.34 m/s). It offers a sufficient timeframe for the nozzles to operate at their natural spray angle, determined by a specific pressure setting. Simultaneously, the duration is appropriate

to prevent over-saturation of the brown paper, ensuring accurate analysis of the area using machine vision techniques. Striking this balance allows for effective evaluation while aligning with realistic field conditions and the capabilities of the robotic smart sprayer platform.

For each pressure and height setting, the nozzle was initially triggered for 2-3 s to mitigate potential inconsistencies in the spray pattern arising from bubble formation in the pipes. Following this initial activation, the nozzle underwent two subsequent 100 ms activations on brown sheets of paper to check for consistency of spray by visual inspection. In the third and final attempt, a new brown paper measuring 88.9 cm by 63.5 cm was used for actual image capture and analysis. This sequential approach aimed to ensure comprehensive observation and analysis of the spray characteristics under varying pressures.



a) b)

Figure 2. Experimental setup for the static – stationary effect test for spray characteristic evaluation. Two 15° and two 25° nozzles activated together (a). Test setup with brown paper underneath the nozzles (b).

b. Static test - wind effect

Frequent winds in agricultural fields pose a significant challenge to nozzle spray applications, potentially leading to spray drift. The development of a spraying system resilient to varying wind speeds necessitated a comprehensive understanding of the behaviors exhibited by different system configurations, specifically those involving pressure and spray height. In the context of precision spray applications, minimizing drift is paramount to ensuring that the intended herbicide spray reaches its targeted weeds. The mitigation of drift is crucial as it directly correlates with the reduction of potential plant damage and subsequent yield loss.

Experimental setup

The wind tests were conducted inside a workshop area using a high-speed floor fan (Lasko Philadelphia, USA; 20-inch, high velocity 360-degree pivot fan) to simulate the wind effect. To ensure an insulated environment, all tests were performed in a closed setting, preventing external winds from influencing the spray dynamics. The 15° nozzle was fixed on the boom in the same position as the static tests, and the floor fan was placed at 76.2 cm (30 inches) from the boom such that the top rim of the fan matched the height of the tip of the nozzle (Figure 3). The boom height was varied for three different heights: 63.5 cm (25 inches), 76.2 cm (30 inches), and 88.9 cm (35 inches), and each time the fan height was also adjusted so that the top rim of the fan was level with the tip of the nozzle. An anemometer (AIOMEST China; Pro HVAC Anemometer) was used to measure the wind speed at the tip of the nozzle. The fan speed was set to the maximum, which produced a wind speed of 3.57 m/s (8 mph) as measured by the anemometer. This wind speed was maintained throughout all the experiments.

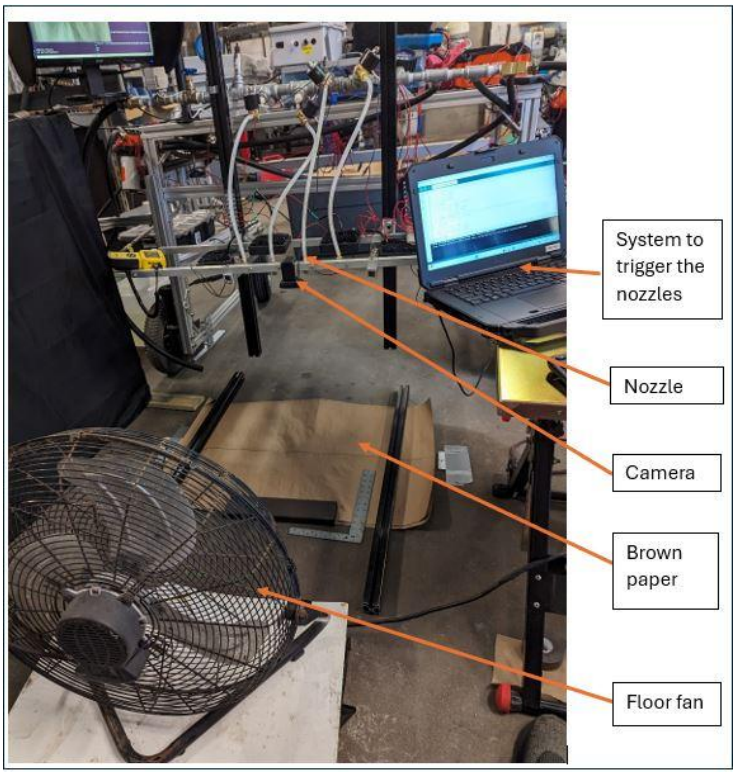


Figure 3. Experimental setup for the fan-based wind test for spray drift evaluation.

The nozzle was triggered for 200 ms to allow ample time for wind to have an effect, as opposed to the 100 ms employed in the static test – stationary effect. Standard brown paper was placed under the nozzle to capture the spray for three different pressure values (aka, 69.95 kPa, 137.89 kPa, and 206.84 kPa). Given the larger spray area observed at 275.79 kPa in the static tests, this pressure was omitted in the wind tests. For each height and pressure combination, the nozzle was activated, and spray patterns were documented. The case with the fan switched on was considered as the 'wind' condition, and the case with the fan off was considered as the ‘no-wind' condition. During image capture, a reference line (e.g., the red line at the image center in Figure 7) facilitated the assessment of relative shifts in spray patterns. To find the relative shift in spray, firstly, the distance between the center line of the spray contour and the reference line is calculated for the ‘no wind’ and ‘wind’ cases. Then the difference in the distance is calculated to find the relative shift in the position of the spray.

For each pressure setting, the nozzle was triggered for 2-3 s, a deliberate measure to mitigate potential inconsistencies in the spray pattern arising from bubble formation in the pipes. Following this initial activation, the nozzle underwent two subsequent 200 ms activations on used brown sheets of paper. In the third and final attempt, a brown paper measuring 88.9 cm by 63.5 cm, featuring a centerline for reference, was utilized to capture the actual spray pattern. This sequential approach aimed at ensuring comprehensive observation and analysis of the spray characteristics under varying pressures.

2.3.2. Dynamic tests

Post completion of static tests, where the effect of pressure and height on the spray area and relative shift in spray position were studied, it was necessary to understand the actual spray behavior at different speeds of the robotic platform while the spraying system was mounted on it. This is different from the wind tests that were conducted with a fan in the previous section, and it is important because it provides a more realistic scenario to evaluate the effect of spray drift, albeit at lower vehicle speeds. In this context, dynamic tests refer to the spray tests conducted with the robotic smart sprayer platform in motion at speeds ranging from 0.45 m/s (1 mph) to 1.34 m/s (3 mph). The objective of the dynamic tests

is to understand the effect of vehicle speed on the spray pattern under varying application pressures for a fixed height. The dynamic tests would help decide the right application pressure and the optimum speed of operation of the robotic smart sprayer platform for achieving the lowest possible spray drift using the 15° nozzle selected (based on the static tests).

Experimental setup

The recommended height of the application based on the static tests was 63.5 cm. While it would be the preferred height for actual spray application in the final prototype, it was decided to use 88.9 cm as the height for the dynamic tests. This is to understand the spray drift in the worst-case scenario. This height was chosen for the tests as it is the height where we would expect to see the maximum effect of spray drift.

A continuous roll of brown paper was placed in a wind-sheltered area, serving as the canvas for the nozzle sprays. The robotic smart sprayer platform traversed over the brown paper and sprayed after a certain pre-determined delay. A TRAM marine GPS receiver (TRAM, Taiwan) was used with a Kalman filter for measuring the speed of the robotic smart sprayer platform. The speed accuracy of the GPS was validated using an average of three trials of moving the robot from point A to point B with a fixed input from the remote-control transmitter stick. This setup allowed for the attainment of a stabilized speed over a considerable distance before reaching the brown paper, ensuring optimal conditions for spray activation. The spray characteristics (spray area and spray length) were evaluated for three different application pressures - 69.95 kPa (10 Psi), 137.89 kPa (20 Psi), and 206.84 kPa (30 Psi). The tests were conducted at three different vehicle speeds – 0.45 m/s, 0.89 m/s and 1.34 m/s. It was determined through preliminary trials that speeds over 1.34 m/s were unsuitable for object detection, thus rendering them impractical for actual field trials. Multiple trial runs were conducted for each speed to verify the smooth operation of the sprayer, addressing potential issues like bubble formation, nozzle misfire, and image capture discrepancies. Following the preliminary system checks and trial runs, the final experimental runs were undertaken for each speed, where the nozzle was triggered for 100 ms.

2.4. Spray analysis using machine vision

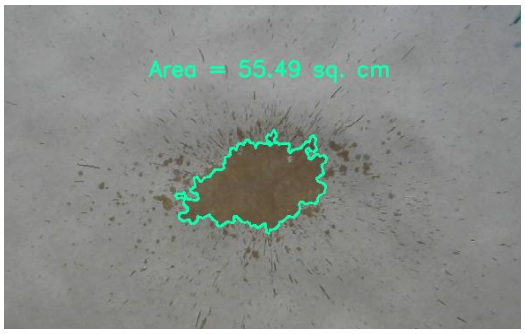
The images from all experiments were captured using a Logitech camera (Logitech Inc., California, USA; C270 HD) positioned on the aluminum tube between the 15° and 25° nozzles to capture their respective sprays. The camera was connected to the Jetson Xavier NX, and a Python program captured the images during the nozzle activation. The spray area's outline was detected using OpenCV's contours detection algorithm. The threshold of the binary mask in the Python code was adjusted to get the right contour that covers the area of the contour completely without including the stray droplets around the main contour. For the static test - wind effect and the dynamic test, the conditions in which the experiments were conducted were in a low light setting during an overcast day, and hence the actual images were comparatively darker. To negate the bad lighting of the images, they were pre-processed to improve the spray region using manual paint and contour marking methods using a software called Inkscape (Harrington et al. 2004 & 2005). Following the manual preprocessing using Inkscape, they were analyzed using Python code. A 90° ruler was placed on the brown paper while the images were captured. This ruler served as the reference object for area calculation from the images captured at each height. The area per pixel was calculated using the image of the reference object and it was subsequently used to calculate the area of the pixels within the spray contour to get the area of the spray.

3. Results

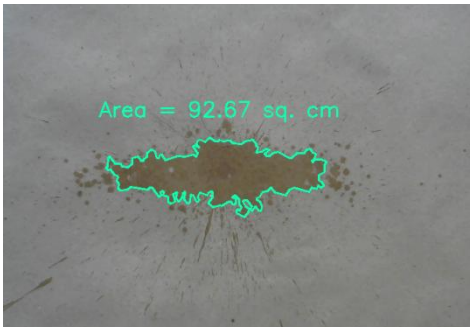
3.1.1 Static test - stationary (no wind) effect

The spray area variation of the 15° and 25° nozzles with a 34.47 kPa increase in pressure is shown in Figure 4. The contour around the spray covered the region where the spray droplets were continuous, thereby forming a main spray region. There were some droplets beyond the main spray region marked by the contour, but they were not included in the spray area calculation as they were discrete and not

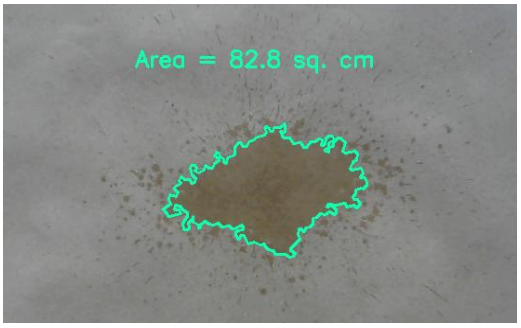
uniform in repeat sprays. Moreover, there were some droplets that were the result of the main spray hitting the brown paper and scattering across. These spray droplet areas were also excluded as they were not part of the main spray region and hence were difficult to be reproduced in the same manner in every trial. The spray area of the 15° nozzle increased linearly from ~22 cm^2 to 275 cm^2 for the 69.95 kPa to 275.79 kPa pressure ranges. Similarly, for the 25° spraying angle nozzle (~70 cm^2 to 275 cm^2 for the 69.95 kPa to 275.79 kPa pressure ranges). The only outlier is the case of 137.89 kPa spray for the 15° nozzle, where the spray area is less than the area of the preceding pressure. This is an outlier considering that for almost all the application pressures for the nozzle types, the spray area increased linearly with pressure. Comparing both the nozzles, the 15° nozzle produces a lower spray area for all the application pressures. In both cases, the spray area increases with application pressure and with increasing spray height.



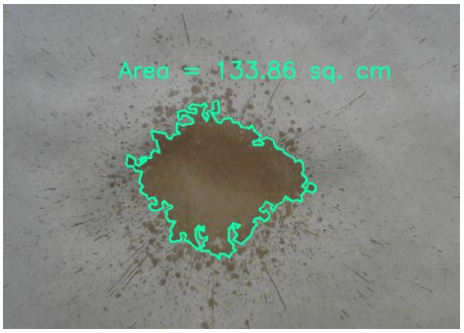
a) 69.95 kPa; 15° nozzle



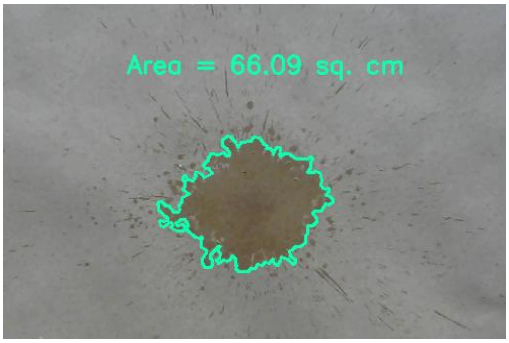
A) 69.95 kPa; 25° nozzle



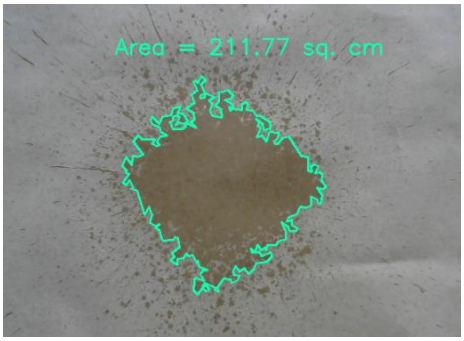
b) 103.42 kPa; 15° nozzle



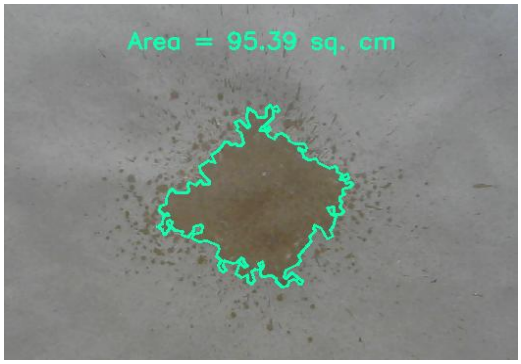
B) 103.42 kPa; 25° nozzle



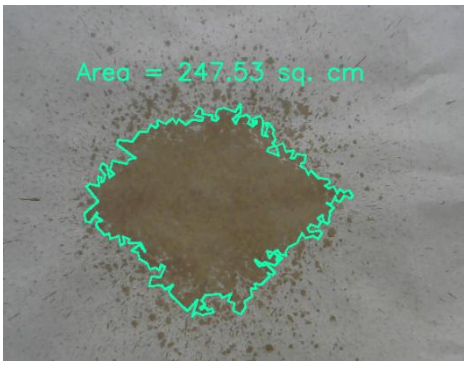
c) 137.89 kPa; 15° nozzle



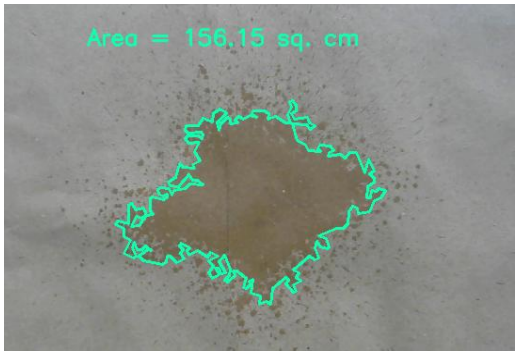
C) 137.89 kPa; 25° nozzle



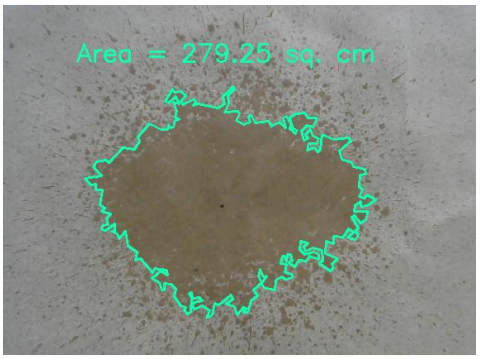
d) 172.37 kPa; 15° nozzle



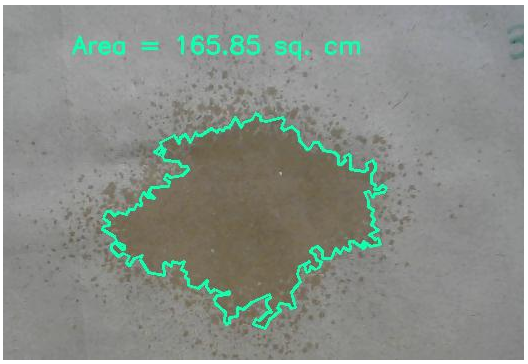
D) 172.37 kPa; 25° nozzle



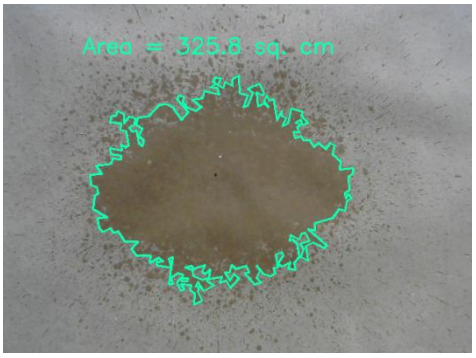
e) 206.84 kPa; 15° nozzle



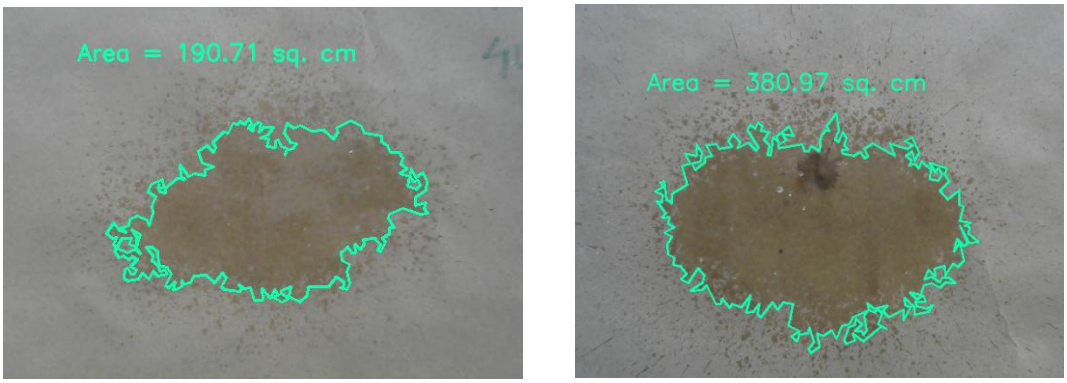
E) 206.84 kPa; 25° nozzle



f) 241.317 kPa; 15° nozzle



F) 241.317 kPa; 25° nozzle



g) 275.79 kPa; 15° nozzle G) 275.79 kPa; 25° nozzle

Figure 4. a) to g) shows the spray pattern of the 15° nozzle at 63.5 cm height from the ground. A) to G) shows the spray pattern of the 25° nozzle at 63.5 cm height from the ground.

Table 2. Spray area for 15° and 25° nozzles at three different heights – 63.5 cm (25 inches), 76.2 cm (30 inches), and 88.9 cm (35 inches) for seven pressure values.

		Spray area (cm^2)						
Height	**Nozzle Angle**	**69.95 kPa**	**103.42 kPa**	**137.89 kPa**	**172.37 kPa**	**206.84 kPa**	**241.317 kPa**	**275.79 kPa**
63.5 cm	15°	55.49	82.8	66.09	95.39	156.19	165.85	190.71
	25°	92.67	133.86	211.77	247.53	279.25	325.8	380.97
76.2 cm	15°	37.97	88.39	127.47	148.15	203.41	233.43	221.63
	25°	155.15	384.56	341.44	442.6	475.19	496.22	565.12
88.9 cm	15°	38.15	136.99	208.04	245.39	289.02	352.37	355.93
	25°	282.88	242.1	356.54	464.22	571.92	617.22	657.48

The results for all the spray area experiments conducted at different spray heights and application pressures for the 15° and 25° nozzles are given in Table 2. Spray width is taken as the distance between the left most point and the right most point of the spray. The variation of the spray width is also the same as the spray area. The spray width variation is presented in Table 3 for the 63.5 cm (25 inch) height as that is the height that produces the smallest area. Therefore, 63.5 cm height is considered the best-case scenario for the spray area and spray width.

Table 3. Spray width for 15° and 25° nozzles at 63.5 cm (25 inches) for seven pressure values.

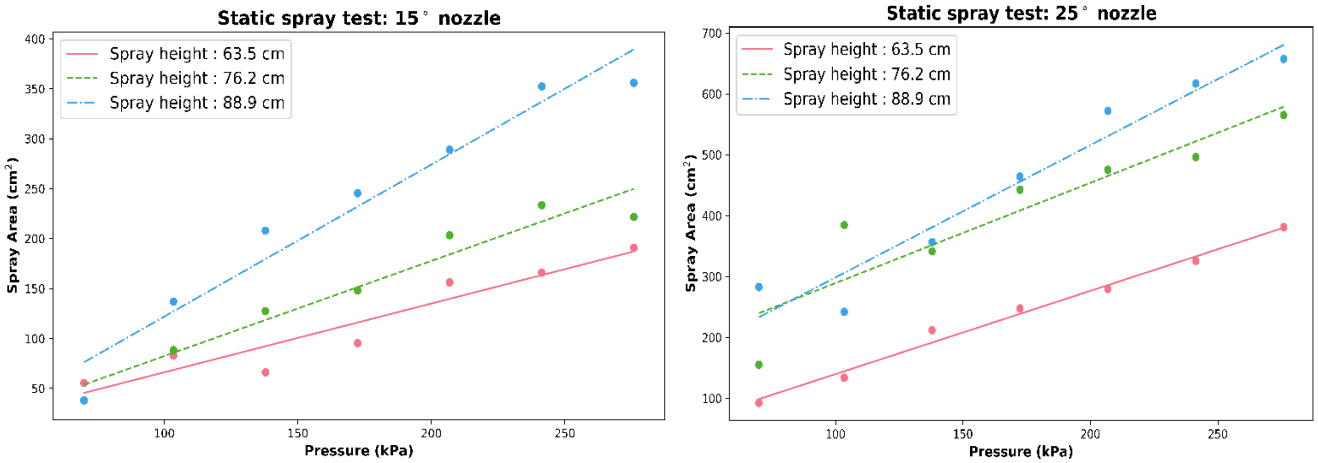
		Spray width (cm)						
Height (cm)	**Nozzle Angle**	**69.95 kPa**	**103.42 kPa**	**137.89 kPa**	**172.37 kPa**	**206.84 kPa**	**241.317 kPa**	**275.79 kPa**
	15°	7.94	9.74	8.98	13.33	15.19	14.85	13.12

63.5 cm	25°	7.8	14.5	20.51	18.37	19.34	21.55	21.34

Statistical analysis

A multiple linear regression analysis is required to understand the statistical significance of the test factors (pressure and height), in this case. This needs a linearity check of the data for spray area variation with pressure for different heights to make sure that linear regression can be applied. To perform the linearity test, a scatter plot was developed for the data for 15° and 25° nozzles. Using a linear model for the spray area data for both nozzles, regression plots were created (Figure 5). The X-axis represents the spray pressure in kPa, while the Y-axis represents the spray area in cm^2. The linear regression line is plotted for all three heights (63.5 cm, 76.2 cm, and 88.9 cm) using R Studio (Posit Software, USA).

The spray area data was flattened to include dummy variables for the heights and pressures. Spray area is the dependent variable, while the heights and pressures were taken as the independent variables. The dependent variable's skewness was estimated to check the normality of the data. The skewness value was -0.6099, which lies within the acceptable skewness range of [-1,1]. Hence, no data transformation was applied to convert the spray area to normalized data. For the 15° nozzle, the analysis of variance (ANOVA) gave a p-value of 1.86×10^{-5} indicating a good level of significance of the model. The R^2 squared value obtained was 0.919. The adjusted R^2 value, which is adjusted for the number of independent variables, was obtained to be 0.866. Both the values are close (only 5% variation), indicating that all the variables included in the model do not massively affect the precision of the prediction.



a) 15° nozzle b) 25° nozzle

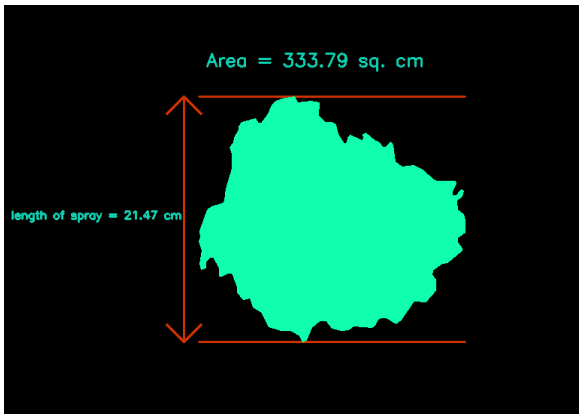
Figure 5. Linear regression line for the two nozzle types for spray area variation vs pressure.

The collinearity of the independent variables was also checked using the variance inflation factor (VIF), which measures multicollinearity in regression. The VIF obtained for the independent variables belonging to height and pressure were less than 1.5, which is acceptable for a strict collinearity check. Hence, we can rule out multicollinearity among the independent variables of pressure and height. For the 25° nozzle, the analysis of variance (ANOVA) gave a p-value of 3.52×10^{-5} indicating a good level of significance of the model. Like the 15° nozzle, the small difference between the R^2 value and the adjusted R^2 value indicates that the variables included in the model aptly predict the spray area.

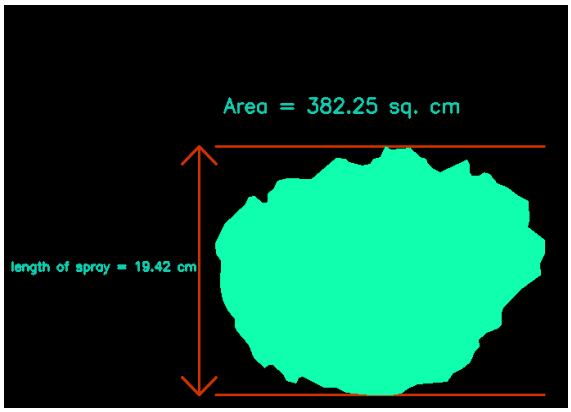
Through the static test – stationary effect, the higher range of pressures (> 206.84 kPa) and the relatively wider-angle nozzle (i.e., the nozzle with a spraying angle of 25°) were eliminated as their spraying characteristics at a stationary state of the vehicle were undesirable. Hence, for the wind effect test and dynamic tests, the focus is on lower pressures for the 15° nozzle.

3.1.2 Static test - wind effect

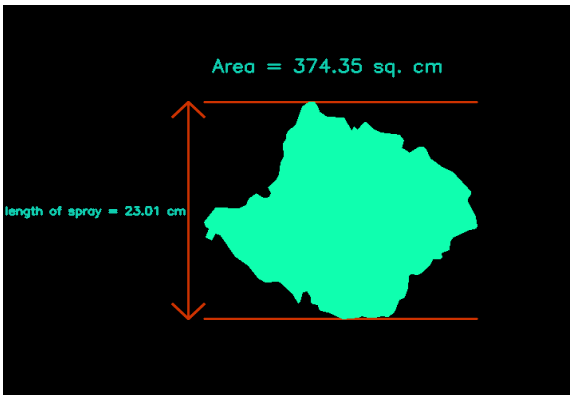
Table 4 shows the spray area of the 15° nozzle at three different spray heights (63.5 cm, 76.2 cm, and 88.9 cm). The spray length is the distance from the topmost point of the spray to the bottom most point of the spray. The spray length was measured from the images (Figure 6), and the corresponding values are shown in Table 4. Figure 6 shows the masks of the spray contours on a black background (colored in a way to highlight the spray area) with the spray length shown for 206.84 kPa activation pressure at three different heights under 'wind' and 'no-wind' conditions.



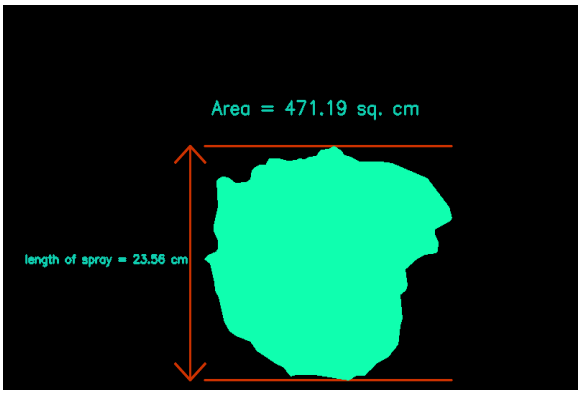
a1. Height: 63.5 cm; 'no wind'



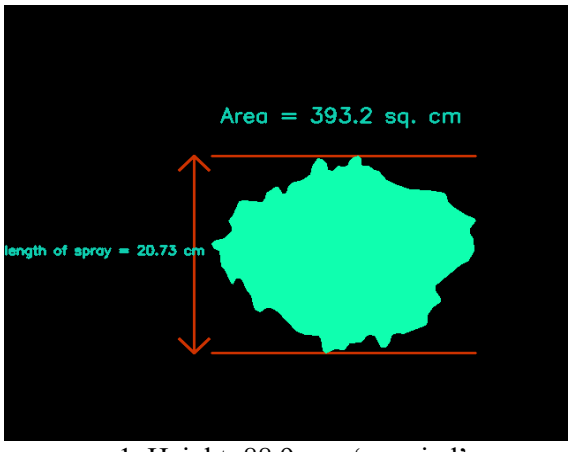
a2. Height: 63.5 cm; 'wind'



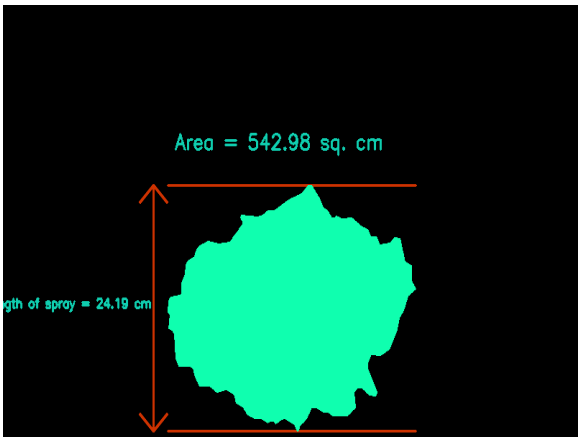
b1. Height: 76.2 cm; 'no wind'



b2. Height: 76.2 cm; 'wind'



c1. Height: 88.9 cm; 'no wind'



c2. Height: 88.9 cm; 'wind'

Figure 6. Spray from the 15° nozzle for 63.5 cm, 76.2 cm, and 88.9 cm height. a1, b1 and c1 are the sprays under the 'no-wind' condition while a2, b2 and c2 are the sprays under the 'wind' condition. All the cases are at 206.84 kPa pressure and area shown.

The area for each height is higher in the 'wind' condition than in the 'no wind' condition. The length of the spray is also higher in the 'wind' condition for all the cases. For the case of 206.84 kPa pressure, the area of spray increases with an increase in height for both 'wind' and 'no wind' cases. This is expected to some extent since the spray spreads out to the bottom as the application height (or boom height) increases.

Table 4. Wind test results (spray area and spray length) for each pressure and height of boom for the 15° nozzle.

Height (cm)	Spray area (sq. cm)						Spray length (cm)					
	69.95 kPa		137.89 kPa		206.84 kPa		69.95 kPa		137.89 kPa		206.84 kPa	
	No wind	Wind	No wind	Wind	No wind	Wind	No wind	Wind	No wind	Wind	No wind	Wind
63.5	62.95	63.8	215.54	311.25	333.79	382.25	8.32	10.7	16.58	18.76	21.47	19.42
76.2	75.32	127.77	247.58	311.35	374.35	471.19	9.71	18.47	19.26	22.37	23.01	23.56
88.9	67.51	103.56	276.16	362.19	393.2	542.98	8.15	12.67	21.18	22.59	20.73	24.19

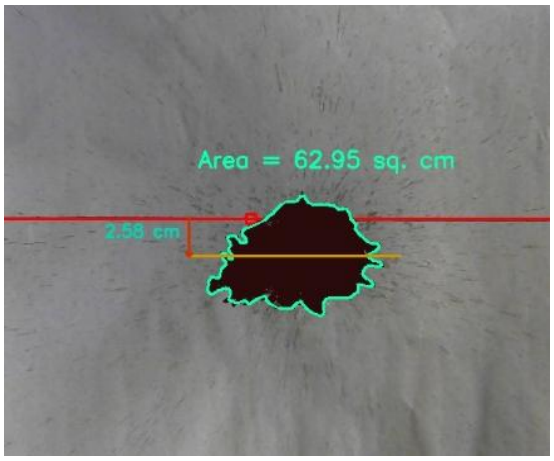
Figure 7 shows the shift in the position of the spray under 'wind' conditions. The distance of the center of the spray was measured from the reference line, and the relative shift in position of the spray under 'wind' and 'no wind' conditions was calculated. This test measures the drift of spray from a 15° nozzle using the center of the spray contour at each studied height and three different pressures. Table 5 details the distance from the reference line for all pressures and heights. The 'wind' and 'no wind' columns show the distance of the center of the spray from the reference line, while the 'shift in position' column is the relative shift of the spray measured as the difference of the distance from the reference line of the 'no wind' and 'wind' cases.

Table 5. The distance from the reference line and the relative distance for the 15° nozzle for each pressure and height setting.

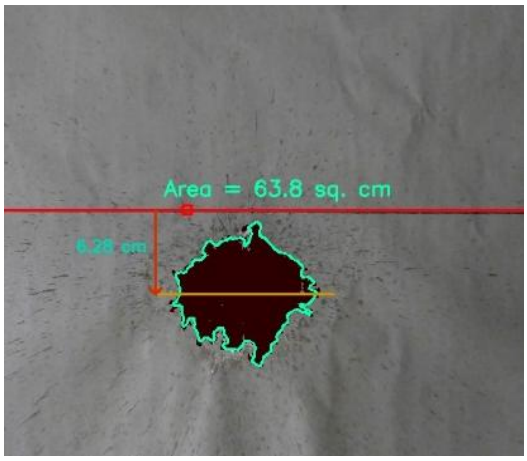
Height (cm)	Distance from the reference line (cm)								
	69.95 kPa			137.89 kPa			206.84 kPa		
	Wind	No wind	Shift in position	Wind	No wind	Shift in position	Wind	No wind	Shift in position
63.5	6.28	2.58	-3.7	9.38	2.51	-6.87	9.05	0.79	-8.26
76.2	13.06	0.32	-12.74	10.91	1.11	-9.8	11.07	-0.24	-11.31
88.9	12.32	5.76	-6.56	13.65	6.56	-7.09	13.82	5.23	-8.59

Multiple linear regression analysis was performed, like the static test (stationary effect). The R^2 value obtained was 0.968, indicating that 96.8% of the variance of the dependent variable (spray area) can be explained by the independent variables ('wind' condition, spray height, and application pressure). The adjusted R^2 value, which is adjusted for the number of independent variables, was obtained to be 0.954. The p-value for the model was 1.53×10^{-8}, indicating a high significance of the independent variables in determining the output of the dependent variable. The coefficients of the pressure variables were substantially higher than the coefficients of the height and 'wind' condition variable, indicating a higher influence of the pressure on the spray area as compared to the wind and spray height conditions.

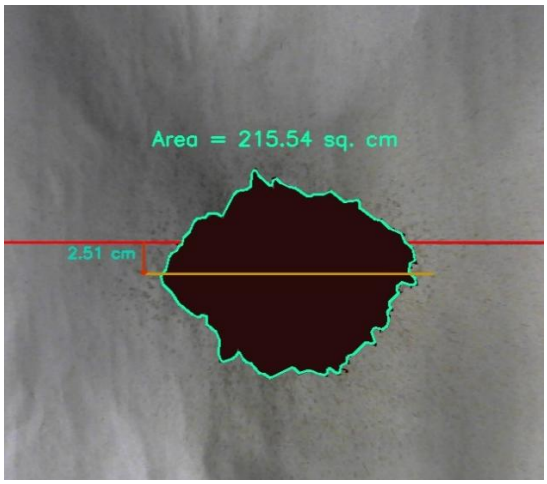
For the spray length variation, a similar analysis was performed, and a p-value of 5.55 x10^{-6} establishes a high significance of the model. An R^2 value of 0.913 shows that the independent variables explain 91.3% of the variation in the spray length. However, unlike the spray area, the spray length coefficients are in the same order of magnitude, indicating that no specific variables are dominating the influence on spray length.



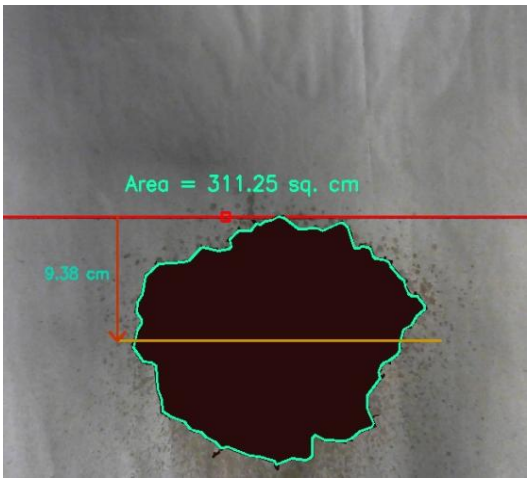
a1. 69.95 kPa; 'no wind'



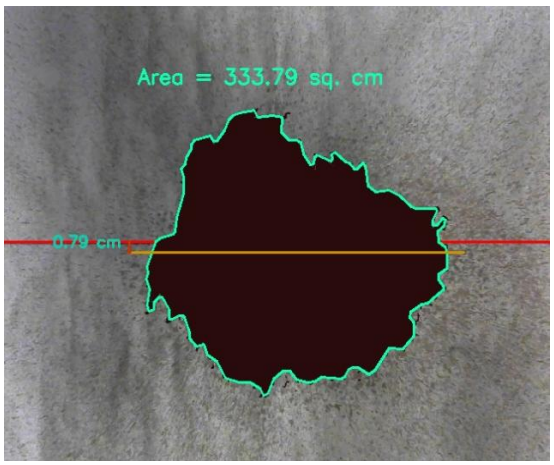
a2. 69.95 kPa; 'wind'



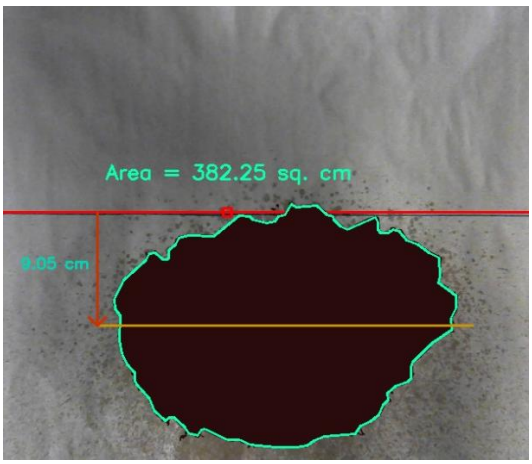
b1. 137.89 kPa; 'no wind'



b2. 137.89 kPa; 'wind'



c1. 206.84 kPa; 'no wind'



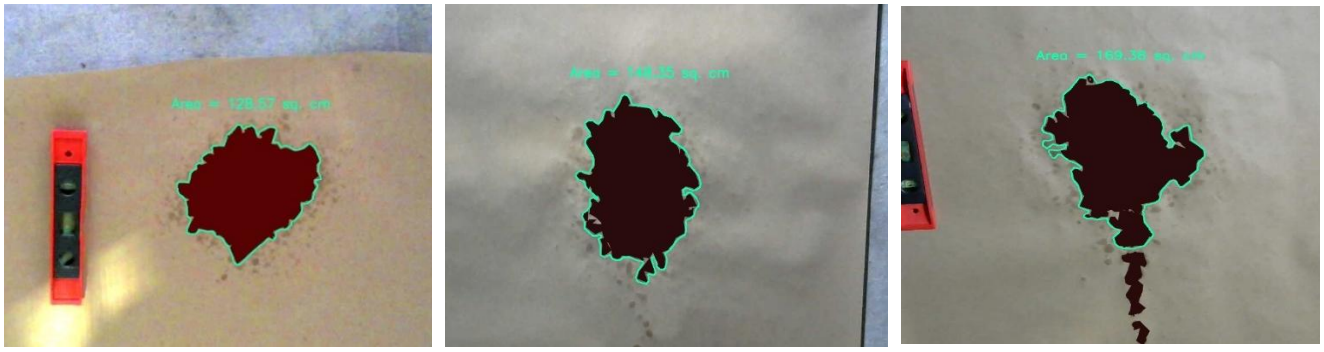
c2. 206.84 kPa; 'wind'

Figure 7. Shift in the position of spray due to wind at different pressures. a1, b1, and c1 are the sprays under the 'no wind' condition, while a2, b2, and c2 are the sprays under the 'wind' condition. All the cases are for sprays from 63.5 cm in height.

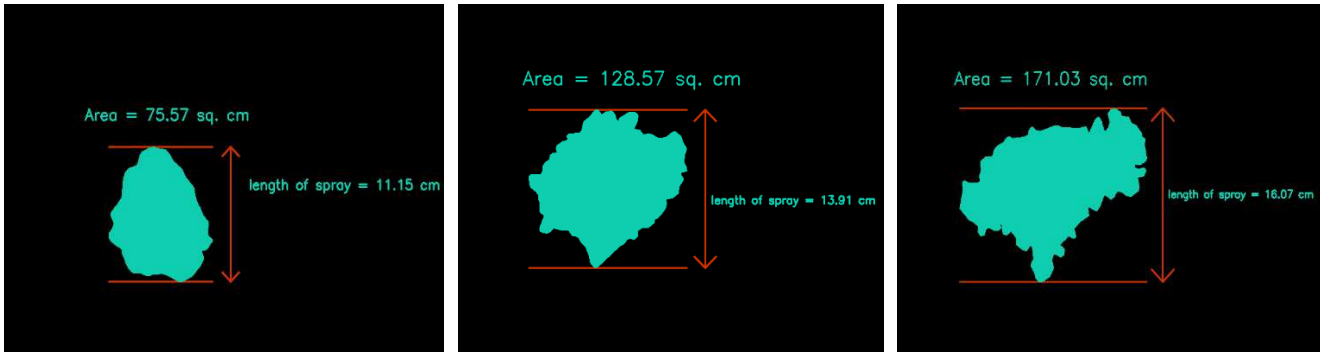
3.2 Dynamic tests

Since the height of the spray application remained constant in this test at 88.9 cm, the focus was to understand the variation of the spray area and spray length under different speeds for different pressures. This would help identify the 'safe speeds' and 'safe application pressures' that would offer the most resistance to drift and have the least potential to cause off-target sprays in the field.

The spray area and length variation with speed for different pressures are presented in Table 6. For each pressure, as the speed increases, the spray area and the length of the spray also increases. Additionally, for each speed, the spray area and length also increase with the increase in pressure. This is like the spray area trend seen for the static test -wind effect. Figure 8 (a – c) shows the variation of the spray area for the same pressure (137.89 Kpa) at incremental speeds of 0.45 m/s, 0.89 m/s, and 1.34 m/s and at the same speed (0.45 m/s) for incremental pressures of 69.96 Kpa, 137.89 Kpa, and 206.84 Kpa (Figure 8, d – f), shown on a black background post-binary mask with the contour highlighted with a cyan color. With the pressure constant, the spray area increases with an increase in speed as seen in Figure 8 (a – c) and Table 6. This is also true for the variation in spray length, which shows an overall trend of increasing values with an increase in speed. The spray length (shown in Figure 8, d – f) increase would mean an increase in the drift of spray with increasing vehicle speeds. With the speed constant and pressure increased, the spray area and spray length also increased for almost all the cases. This behavior is consistent with the spray area increase seen with pressure increase in the wind tests and static tests.



a. 137.89 kPa 0.45 m/s b. 137.89 kPa 0.89 m/s c. 137.89 kPa 1.34 m/s



d. 69.95 kPa 0.45 m/s e. 137.89 kPa 0.45 m/s f. 206.84 kPa 0.45 m/s

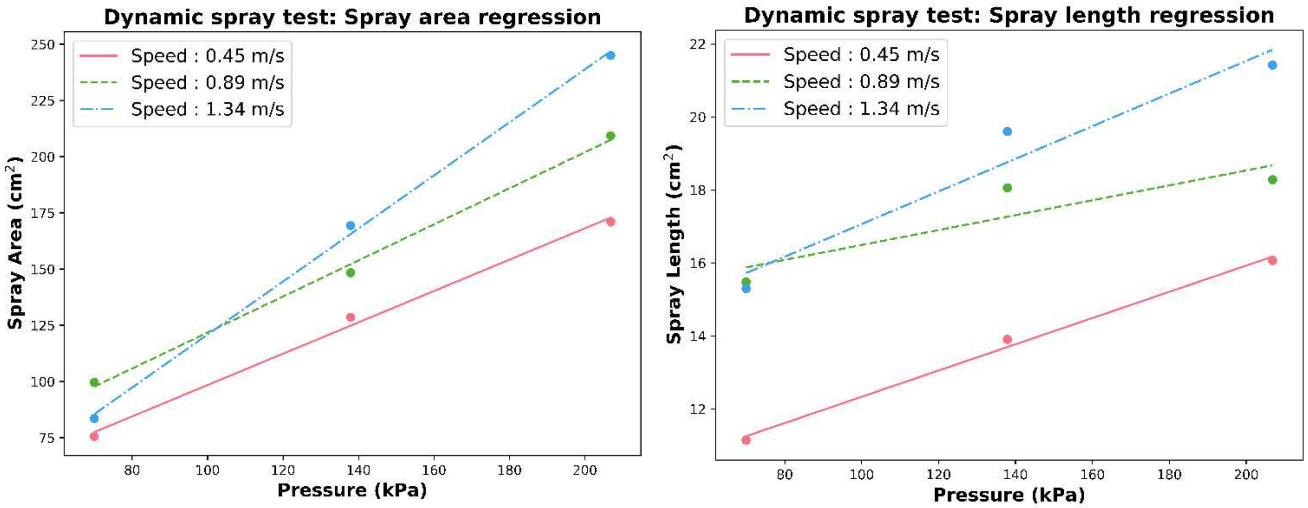
Figure 8. The effect of the speed of the robotic platform on the spray area and spray length at 137.89 kPa (a to c) and at different pressures for the same speed of 0.45 m/s (d to f).

Table 6. Spray area and spray length calculation for the 15° nozzle mounted on the robotic platform moving at different speeds for different operational pressures.

Speed (m/s)	Spray area (sq. cm)			Spray length (cm)		
	69.95 kPa	137.89 kPa	206.84 kPa	69.95 kPa	137.89 kPa	206.84 kPa
0.45	75.57	128.57	171.03	11.15	13.91	16.07
0.89	99.61	148.35	209.30	15.48	18.06	18.28
1.34	83.53	169.38	245.01	15.30	19.60	21.42

Linearity tests were performed using a scatter plot for the data for spray area and spray length data. Using a linear model, regression plots were created. The X-axis represents the spray pressure in kPa, while the Y-axis represents the spray area (Figure 9 (a)) and spray length (Figure 9 (b)). The linear regression line was plotted for all three speeds – 0.447 m/s, 0.894 m/s, and 1.341 m/s using R studio. The skewness of spray area (0.35) and spray length (-0.18) were within the acceptable limits indicating good normality of the data. The p-values for both the spray area (0.0012) and spray length (0.002) variation are within the α value of 0.05 and therefore is significant. For the spray area, the R^2 value for the spray area variation is 0.948 with an adjusted R^2 of 0.917 to account for the independent categorical variables. Lower difference between the R^2 and the adjusted R^2 is favorable for the model. For the spray length variation, high values for R^2 (0.931) and adjusted R^2 (0.889) were observed. A p-value of 0.0024 indicates that the effect of the independent variables (speed and pressure) on the dependent variable (spray length) is statistically significant.

The statistical tests for the experiments from the static tests – with and without wind, and the dynamic test prove that the independent variables (speed, application pressure, spray height, wind) have a significant effect on the dependent variables (spray height and spray length). A model involving these independent variables would be able to explain a big portion of the variance of the dependent variable.



a) Spray area variation b) Spray length variation

Figure 9. Linear regression line for the 15° nozzle for spray area variation (a) and spray length variation (b) vs pressure.

4. Discussion and Challenges

4.1.1 Static tests – stationary (no wind) effect

The spray area and spray width are important parameters in determining the right nozzle type, height, and pressure range, as they provide a starting point for narrowing down the operational range of these variables. As is observed from Tables 2 and 3, increasing the height of the spray increases the spray area and spray width. It is interesting to note that beyond a certain point, a reduction in coverage density could be seen because of finer sprays being produced as pressure is increased. As a result, lower pressures and lower spray heights are the preferred settings for the nozzles, as the spraying system achieving a smaller spray area is a critical objective of the robotic smart spraying system. Lower spray area and spray width would facilitate spraying on smaller weeds without affecting the nearby plants, provided spray drift is controlled.

Using the spray width, the total horizontal length (the horizontal field of view), and the percentage overlap, the minimum number of nozzles required to cover the whole intended area for the smart spraying application is calculated (equation 1). A 100 % overlap is achieved when the edge of the spray from one nozzle intersects the mid-point of the width of the spray from the adjacent nozzle (Wolf, 2019). The total horizontal length for the robotic smart sprayer includes the width of the raised bed and a small area on either side to account for the weeds on the edges. For the current setup, it is equal to a horizontal field of view of 106.68 cm (42 inches).

$$\textbf{Minimum number of nozzles required} = \frac{\textbf{Total horizontal length}}{\textbf{Spray width} * (\mathbf{1} - \textbf{\% overlap})} \qquad \textbf{(1)}$$

Using the spray width data provided in Table 2 and applying equation 1, the estimated number of nozzles for each pressure was calculated, as detailed in Table 7. The determination of the ideal percentage overlap relies on the specific application. Opting for a higher percentage overlap may result in double spraying of a plant between two smaller weeds if adjacent nozzles are activated. For a precision spraying application, where minimizing the herbicide sprayed on non-target areas is crucial, a lower percentage overlap (0-10%) is preferable. Based on the analysis of spray area and width in the static tests, the 25° nozzle can be confidently excluded from further consideration. This decision is supported by its consistent generation of a much larger area compared to the 15° nozzle. Additionally, higher pressures (>172.37 Kpa) and spray heights (>76.2 cm) can be excluded, as they exhibit similar issues, aligning the selection with more effective and precise spraying parameters.

Table 7. Estimated number of nozzles required based on the spray length, required horizontal FOV, and application pressure.

Nozzle Angle	Percentage Overlap	Minimum number of nozzles						
		69.95 kPa	103.42 kPa	137.89 kPa	172.37 kPa	206.84 kPa	241.317 kPa	275.79 kPa
15°	0 %	13	11	12	8	7	7	8
	5 %	14	12	13	8	7	8	9
	10 %	15	12	13	9	8	8	9
	15%	16	13	14	9	8	8	10
	20%	17	14	15	10	9	9	10

25°	0 %	14	7	5	6	6	5	5
	5 %	14	8	5	6	6	5	5
	10 %	15	8	6	6	6	6	6
	15%	16	9	6	7	6	6	6
	20%	17	9	7	7	7	6	6

4.1.2 Static test - wind effect

Spray area increases proportionally with an increase in application pressure, concurrent with an elevated flow rate. Figure 7 illustrates a similar trend for all the studied spray heights, wherein, at a specific pressure, the ‘wind’ configuration exhibits a larger spray area than the ‘no wind’ case. This behavior is anticipated at wind speeds of 3.57 m/s, wherein the force disperses smaller droplets in the lower half of the spray, resulting in a broader coverage. The general trend, observable in both 'wind' and 'no wind' cases, indicates an increased spray area with an increase in boom height/spray height, as depicted in Figure 8 for pressures of 137.89 kPa and 206.84 kPa. This aligns with expectations, given that increased height correlates with a heightened spray angle, causing the spray to disperse more widely.

However, the spray area at 69.95 kPa does not conform to this trend (Figure 10). Specifically, at 76.2 cm, the 'wind' and 'no wind' conditions exhibit a higher spray area than at 88.9 cm. This deviation could potentially be attributed to cavitation effects (bubble formation in the solenoid to nozzle pathway) at lower pressure, influencing flow dynamics at certain boom heights, or minor variations in temperature and humidity impacting the spray under lower pressure. It is worth noting that, despite efforts to regulate the experiment environment by closing the workshop to external airflow, limitations persisted due to the constraints of the workshop building. Another plausible explanation is the restricted size of the floor fan employed for the experiment, a 50.8 cm high-velocity floor fan. While efforts were made to align the top rim of the fan with the nozzle tip across different heights (63.5 cm, 76.2 cm, and 88.9 cm) for consistency, it might not have covered the entire height of the spray in the 88.9 cm case due to diameter limitations. This effect is more pronounced in the 69.95 kPa case, given its coarser droplets. Consequently, the full impact of a 3.57 m/s wind may not have presented in the 88.9-cm case for 69.95 kPa, unlike the 137.89 kPa and 206.84 kPa scenarios where finer droplets are more prone to drifting, even without a direct wind in their path. Consequently, the expected behavior of a larger spray length at 88.9 cm compared to 76.2 cm in the 69.95 kPa case is not observed.

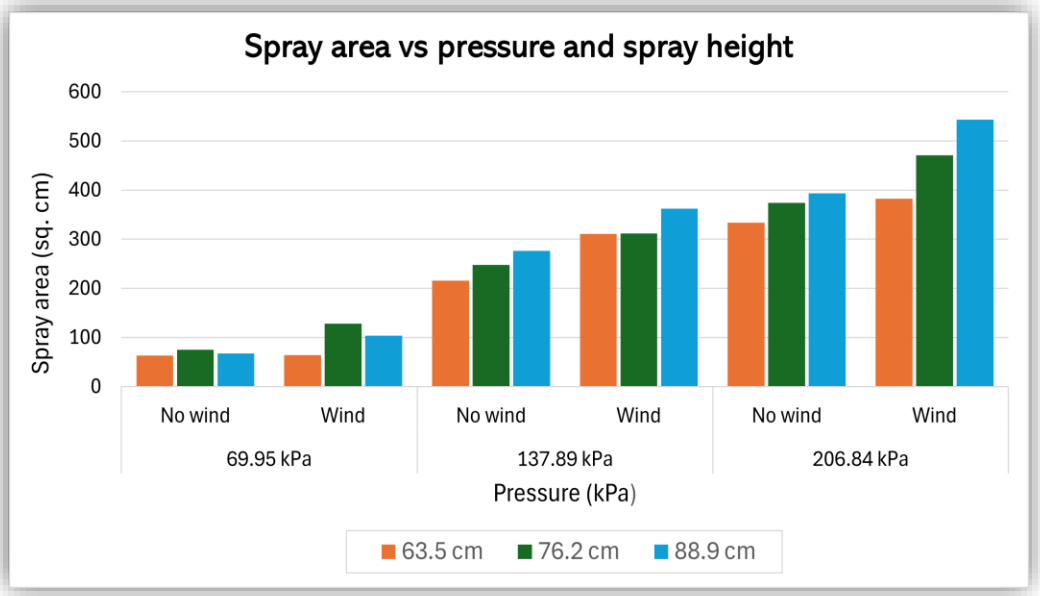


Figure 10: Spray area of the nozzle at 63.5 cm, 76.2 cm, and 88.9 cm spray height under 'wind' and 'no wind' conditions.

The assessment of spray length (Figure 11) at different pressures and spray heights provides insights into drift potential due to wind i.e. how wind speeds influence spray drift in terms of the shift in the spray position. Notably, the 'wind' configuration consistently exhibits a greater spray length than the 'no wind' case across all application pressures and spray heights/boom heights. For the 63.5 cm spray, all 'wind' cases display a higher spray length compared to the 'no wind' instances, except at 206.84 kPa. However, this result is not as significant due to the higher spray area of the 'wind' spray (Figure 10), which still follows the expected trend. Moreover, an increase in pressure corresponds to an increase in spray length for both 'wind' and 'no wind' cases, aligning with expectations of the spray stretching at the bottom half under the influence of wind speeds.

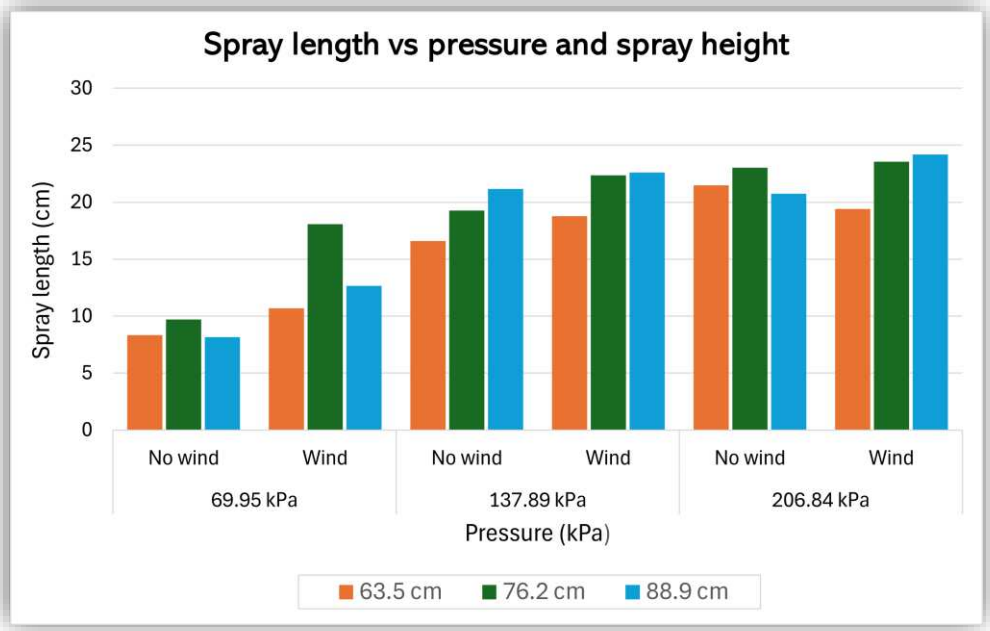


Figure 11: Spray length of the nozzle at 63.5 cm, 76.2 cm, and 88.9 cm spray height under 'wind' and 'no wind' conditions.

It is essential to emphasize that relying solely on the isolated examination of spray length results may be misleading, given the potential for partial information and misinterpretation. For example, consider the scenario of a 206.84 kPa spray at a 63.5 cm height, where the 'wind' spray area exceeded that of the 'no wind' counterpart. Despite this, the spray length in the 'wind' case was shorter than in the 'no wind' case. Therefore, it is advisable to complement the analysis with the spray area chart and the relative shift in spray position chart (Figures 10 and 12) when conducting nozzle spray analysis for studying the influence of wind on spray drift.

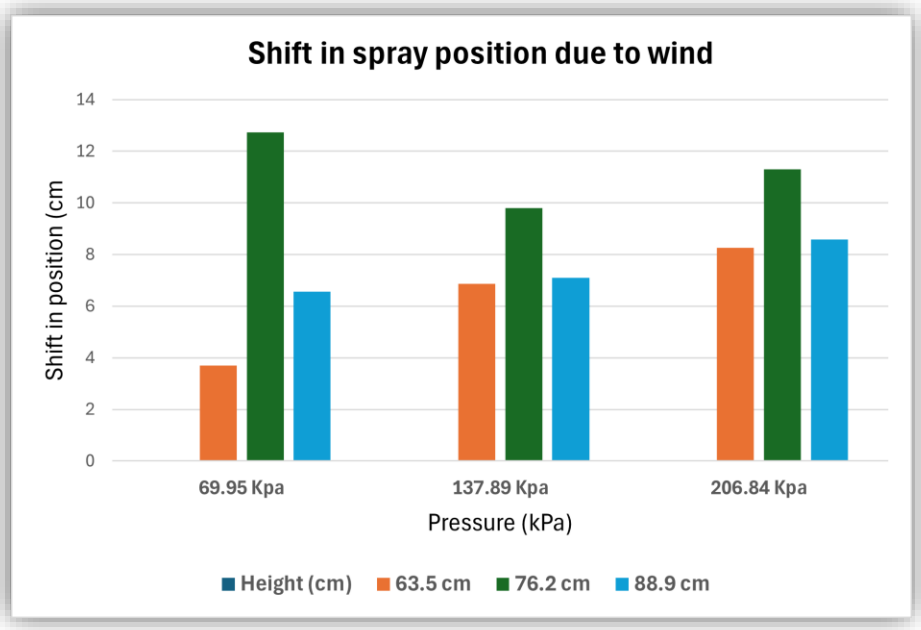


Figure 12: The effect of spray position shifting because of wind ('wind' condition) at different spray heights.

The shift in position of the sprays for different pressure and heights (Figure 12) reveals an interesting pattern. At a spray height of 63.5 cm, the shift in the spray position is higher as the pressure increases. This is because the spray area expands with increased application pressure, resulting in finer droplets. If the spray area and droplet size stayed the same, higher pressure would lead to a smaller shift in position. However, the decrease in droplet size contributes to a higher shift in spray position, even at a low height of 63.5 cm. In theory, one would expect a greater shift in position for smaller pressures, like 69.95 kPa, as the spray application height increases. Consequently, the shift in position at 76.2 cm and 88.9 cm is higher than 63.5 cm. However, the limitations of the floor fan used might have affected the shift of sprays at the 88.9 cm height, where we would expect a larger shift than observed at 76.2 cm.

The major conclusions drawn from the wind test are based on the observations of the variation of spray area and the shift in spray position. Not only do we establish the expected result of lower spray heights/boom heights being preferable to minimize drift and ensure a smaller spray area, but also quantify the actual shift in the spray under the effect of wind for different pressures and heights. Through calculations of spray area and spray length, the relative change in spray length and the position of the center of the spray could be determined. For the current setup, a spray height of 63.5 cm is recommended.

Application pressures significantly impact the spray area and drift resistance. For the lowest height tested (63.5 cm), the shift in spray position increases with increase in pressure, contrary to the expected notion of higher pressures being objectively better resistant to drift. This behavior occurred possibly because of the presence of finer sprays as the pressure increased leading to higher drift. The

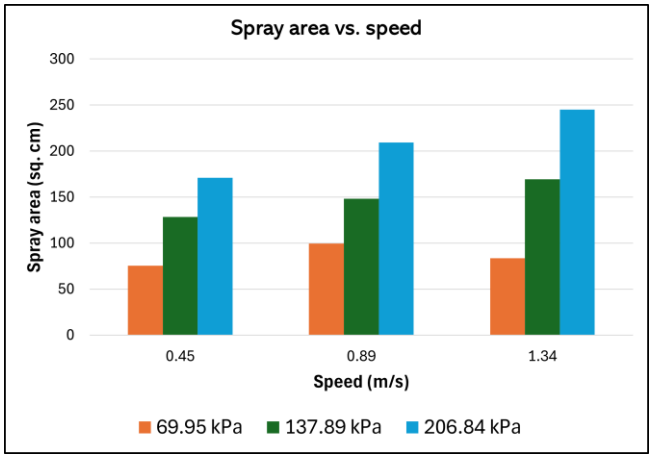
lower pressure spray had coarser droplets and at the lowest height, it was more resistant to drift. To minimize the spray drift at lower height of application, a lower pressure (i.e., 69.95 kPa – 137.89 kPa) setting is advisable. The appropriate application pressure within this range would depend on the droplet size for the application, as different weed types require specific droplet sizes. Additionally, the selected pressure should offer enough wind resistance for application times between 100 ms to 1,000 ms.

Off-target drift of herbicides on to plants causes the spray to miss the intended target (aka, weeds), either partially or completely, and spray on the plants, causing them damage. The resistance to wind for a spray is important as it would reduce off-target drift during field applications. Off-target sprays would also result in the wastage of herbicide and might result in spray deposition on the soil next to the raised beds. The wind experiments in this section were conducted for an application time of 200 ms. For longer application times, it might be better to choose a pressure slightly higher than 69.95 kPa, despite its optimal performance in terms of the smallest spray area achieved and the shortest shift in position under wind effects for 200 ms activation time.

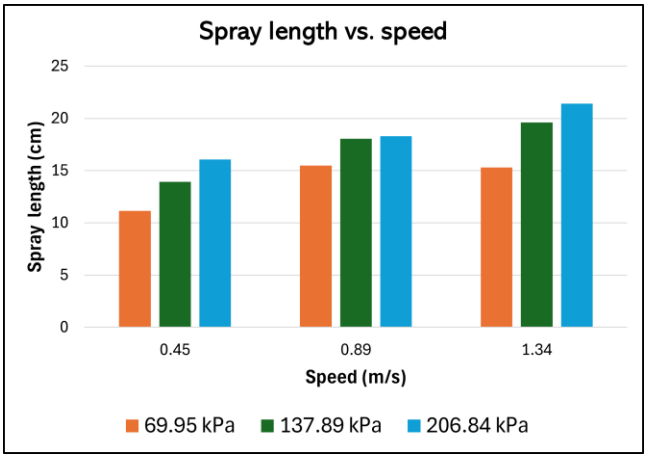
4.2 Dynamic tests

Examining how the speed of the robotic smart sprayer platform affects spray area and length provides valuable insights into determining suitable operational speeds for spraying with the current robotic setup and chosen nozzle. Typically, robotic platforms in field applications operate at lower speeds, usually under 2.2 m/s (Shapiro et al., 2009; Jat et al., 2023), compared to conventional farming vehicles, which usually range from 1 to 4 m/s. In the case of spot spraying or variable rate applications, restrictions on vehicle speed are influenced by the machine vision system. In our specific setup, limitations imposed by both the machine vision system and the robotic platform led us to investigate spray drift at speeds of 0.45 m/s, 0.89 m/s, and 1.34 m/s. Despite the relatively low speeds, the observed spray patterns exhibited similar behaviors to previous tests.

An interesting observation is that both spray area and length increase with higher speeds at the same pressure (Figure 13). Moreover, the rise in spray area per unit speed is more pronounced with increasing pressure. This implies that lower pressures are likely to exhibit a smaller increase in drift with rising vehicle speeds. The common expectation might have been that lower-pressure sprays would be less resistant to vehicle speeds, potentially struggling to withstand spray drift as effectively as higher-pressure sprays. However, it's crucial to consider droplet size and spray angle in this context. The nozzle characteristics indicate that the spray angle linearly increases with pressure up to 275.79 kPa (Supplementary Figure S1a). Additionally, as pressure increases, droplets become finer. Consequently, both spray area and length experience an increase, although the coverage density decreases as the number of finer droplets increases with increasing pressure. This dual effect of pressure on spray characteristics adds nuance to the expected relationship between pressure, vehicle speed, and spray drift.



a)



b)

Figure 13: Variation of spray area (a) and spray length (b) vs. speed of the robotic smart sprayer platform.

At higher speeds, a trailing element or 'tail' was observed in the spray pattern (Figure 14) when the vehicle speed approached 1.34 m/s at both 137.89 kPa and 206.84 kPa. This phenomenon occurs because, upon nozzle closure after activation, the last part of the spray released lags the initial spray point. Even though the nozzles are expected to close immediately after the signal is sent, there is still some latency in the opening and closing of the solenoid valves. This causes a delay, which results in a small percentage of spray droplets releasing in this period. The presence of 'tail' is more pronounced at higher speeds as the speed of the robotic sprayer causes the droplets in the 'tail' area to be spread out more, as compared to the smaller speeds (< 0.89 m/s). where it is more concentrated closer to the main spray region. The 'tail' portion of the spray was not factored into the actual spray length calculation. The inconsistency in the 'tail portion' across trials made it challenging to establish a consistent pattern for interpreting results related to spray length and area. Despite this, acknowledging the presence of the 'tail' is crucial when assessing spray characteristics at different speeds for 137.89 kPa and 206.84 kPa, as it contributes to spray drift. Its impact may increase with prolonged nozzle activation, particularly at higher speeds and pressures.

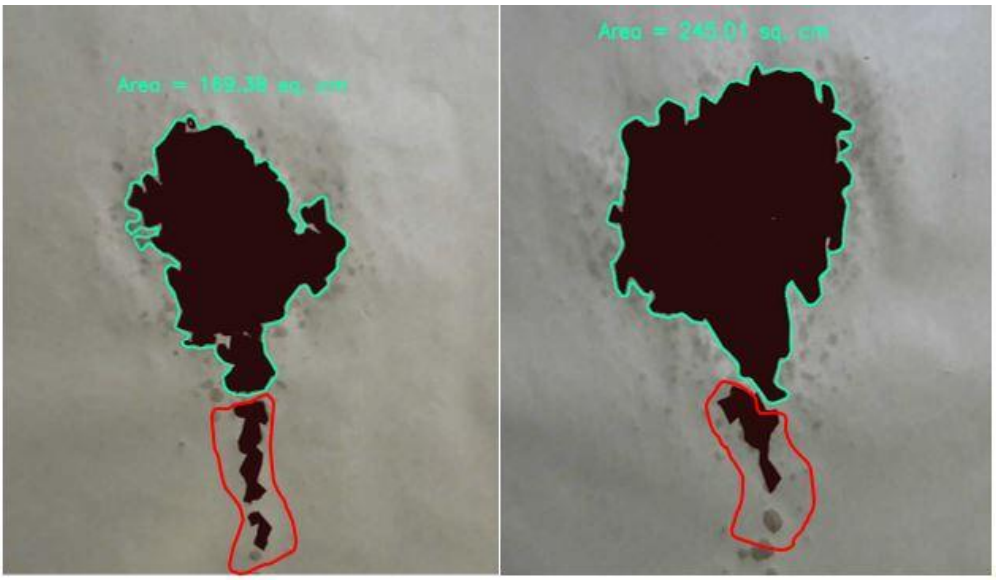


Figure 14. Drift of spray causing an elongated 'tail' element to be formed for 137.89 kPa (left) and 206.84 kPa (right) at 1.34 m/s. The red marked portion is the 'tail' or the lagging element of the spray.

This leads us to the conclusion that operating at speeds less than 0.89 m/s would be preferable to avoid off-target sprays due to spray drift. Also, higher pressures result in the formation of a spray 'tail', which is a collection of larger size droplets that were airborne when the nozzle was shut off and deposited as a trailing element of the spray as the robotic smart sprayer platform moves forward. Tail formation was observed to be more noticeable at higher pressures, making it preferable to implement lower pressures. However, this observation is based on the sprays that we observed for an activation time of 100 ms. In real-time field application, it is possible to encounter multiple weeds in proximity or broad leaf weeds that have a larger spread. This would mean a slightly higher activation time (200 – 500 ms), where we might expect a higher drift from the lower pressure sprays. In such a case, a pressure between 69.95 kPa and 137.89 kPa would be ideal as it would offer a smaller spray area as well as good drift resistance even at higher activation times.

5. Conclusion and Future Work

This study presented a novel, low-cost, machine-vision-based methodology for quantitative spray pattern evaluation and nozzle selection in robotic precision weed sprayers. Unlike conventional approaches that rely on droplet-level measurements or manufacturer specifications, the proposed framework enables direct assessment of spatial spray characteristics, including spray area, width, length, and displacement, under both static and dynamic operating conditions. The robotic smart sprayer platform evaluated in this work serves as a representative case study, demonstrating the applicability and practicality of the proposed methodology for real-world precision spraying systems. Using this framework, two nozzle types (15° and 25°) were systematically evaluated across varying pressures, spray heights, wind conditions, and platform speeds. The results showed that the 15° nozzle consistently produced a smaller spray area and narrower spray width, making it more suitable for targeted weed control applications. Across all tests, spray area and width increased with both spray height and application pressure. Under wind and dynamic conditions, higher pressures led to increased spray displacement due to the formation of finer droplets, highlighting the complex trade-off between coverage and drift resistance. The integrated analysis of static (no-wind and wind) and dynamic experiments enabled the identification of an optimal operating range. A spray height of 63.5 cm and a pressure range of approximately 69.95–137.89 kPa were found to provide a balance between minimizing spray footprint and maintaining drift resistance. Additionally, platform speeds below 0.89 m s^{-1} were shown to reduce spray distortion and prevent the formation of trailing "tail" effects, which can contribute to off-target application. These findings emphasize that optimal performance in precision spraying is governed by the interaction of multiple parameters, rather than any single factor.

Beyond the specific results, the primary contribution of this work lies in the development of a generalizable evaluation framework that can be adapted to different sprayer platforms, nozzle types, and crop systems. The methodology provides a practical tool for data-driven optimization of spraying systems, supporting improved targeting accuracy, reduced chemical usage, and more sustainable weed management practices. At the same time, several challenges were identified. Experimental limitations related to wind simulation, imaging conditions, and platform-specific constraints highlight the need for further validation under field conditions. Additionally, integrating droplet-level characterization and extending the framework to a broader range of nozzles and application scenarios would further strengthen its applicability. Future work will focus on expanding the methodology to include additional nozzle designs (e.g., zero-angle and low-flow nozzles), improving wind simulation and field validation, and evaluating the interaction between spray characteristics and different herbicide formulations. Addressing these challenges will further enhance the robustness and applicability of the proposed framework, contributing to the advancement of precision spraying technologies in smart agriculture.

Acknowledgment

This material was made possible, in part, by a Cooperative Agreement from the U.S. Department of Agriculture, National Institute of Food and Agriculture, Award #2020-67021-30761. Its contents are solely the responsibility of the authors and do not necessarily represent the official views of the USDA.

References

Abdulridha J., Bashyal M., Ampatzidis Y., and Kanissery R., 2023. Steam application with paraquat to control goat weed (Scoparia dulcis) in citrus orchards. Smart Agricultural Technology, 6, 100355, https://doi.org/10.1016/j.atech.2023.100355.

Abdulridha J., Kanissery R., McAvoy C., Ampatzidis Y., 2019. Evaluation of steam application for weed management in citrus groves. Applied Engineering in Agriculture, 35(5), 805-814, doi: 10.13031/aea.13494.

Baltazar, A.R., dos Santos, F.N., Moreira, A.P., Vlente, A., Cunha, J.B., 2021. Smarter robotic sprayer system for precision agriculture. Electronics, 10(17), 2061. https://doi.org/10.3390/electronics10172061

Barbosa Júnior M.D., Moreira B.R.A., Carreira V.S., Brito Filho A.L., Trentin C., Souza F.L.P., Tedesco D., Setiyono T., Flores J.P., Ampatzidis Y., Silva R.P., Shiratsuchi L.S., 2024. Precision Agriculture in the United States: A comprehensive meta-review inspiring further research, innovation, and adoption. Computers and Electronics in Agriculture, 221, 108993, https://doi.org/10.1016/j.compag.2024.108993.

Carbon Robotics: Autonomous LaserWeeder demo Unit. (2022). Carbon Robotics. https://carbonrobotics.com/autonomous-weeder

Chen, H., Lan, Y., Fritz, B. K., Hoffmann, W. C., & Liu, S. (2021). Review of agricultural spraying technologies for plant protection using unmanned aerial vehicle (UAV). International Journal of Agricultural and Biological Engineering, 14(1), Article 1. https://doi.org/10.25165/ijabe.v14i1.5714

Datta, A, and Knezevic, SZ. 2013 Flaming as an alternative weed control method for conventional and organic agronomic crop production systems: a review Adv Agron. 118 399 428. doi: 10.1016/B978-0-12-405942-9.00006-2

Grisso, R., Askew, S. D., & McCall, D. (2019). Nozzles: Selection and sizing. virginia cooperative extension. https://doi.org/10.21061/442-032_BSE-262P

Hofman, V., & Solseng, E. (2004). Spray equipment and calibration. NDSU Extension Service Fargo.

Hunter, J.E., Gannon, T.W., Richardson, R.J., Yelverton, F.H., Leon, R.G. (2020). Coverage and drift potential associated with nozzle and speed selection for herbicide applications using an unmanned aerial sprayer. Weed Technology, 34(2), 235-240. doi:10.1017/wet.2019.101

Hussain, N., Farooque, A. A., Schumann, A. W., McKenzie-Gopsill, A., Esau, T., Abbas, F., Acharya, B., and Zaman, Q. (2020). Design and development of a smart variable rate sprayer using deep learning. Remote Sensing, 12(24), 4091. https://doi.org/10.3390/rs12244091

Jat, D., Dubey, K., Potdar, R. R., Chakraborty, S. K., Kumar, S. P., Chandel, N. S., Rajwade, Y. A., & A, S. (2023). Development of an automated mobile robotic sprayer to prevent workers' exposure of agro-chemicals inside polyhouse. Journal of Field Robotics, 40(6), 1388–1407. https://doi.org/10.1002/rob.22181

Johnson, M.P., & Swetnam, L.D. (1996). Sprayer nozzles: selection and calibration. Lexington: University of Kentucky, 1996. 6 p.

Liu, Y., Mohammadzamani, D., Javidan, S.M., Ampatzidis, Y. (2026). Comprehensive performance analysis of UAV agricultural sprayer under variable conditions: A step towards crop health and precision spraying in next-generation agriculture. Applied Engineering in Agriculture, 42(1). 167-176, https://doi.org/10.13031/aea.16523

Ma, G., Javidan, S.M., Ampatzidis, Y., Zhang, Z. (2026). Towards the development of a robotic spraying arm: AI-based weed detection and path planning strategies. Robotics and Autonomous Systems, 201, 105443. https://doi.org/10.1016/j.robot.2026.105443

Meyer, C.J., Norsworthy J.K., Kruger, G.R., Barder, T.L., 2016. Effect of Nozzle selection and spray volume on droplet size and efficacy of engenia tank-mix combinations. Weed Technology, 2016;30(2):377-390. doi:10.1614/WT-D-15-00141.1

Nuyttens, D., De Schampheleire, M., Baetens, K., Brusselman, E., Dekeyser, D., Verboven, P. (2011). Drift from field crop sprayers using an integrated approach: results of a five-year study. Transactions of the ASABE, 54(2), 403-408. doi:10.13031/2013.36442

Partel V., Costa L., Ampatzidis Y., 2021. Smart tree crop sprayer utilizing sensor fusion and artificial intelligence. Computers and Electronics in Agriculture 191, https://doi.org/10.1016/j.compag.2021.106556

Partel V., Kakarla S.C., and Ampatzidis Y., 2019. Development and evaluation of a low-cost and smart technology for precision weed management utilizing artificial intelligence. Computers and Electronics in Agriculture, 157, 339-350, https://doi.org/10.1016/j.compag.2018.12.048.

Rakhmatulin, I., & Andreasen, C. (2020). A concept of a compact and inexpensive device for controlling weeds with laser beams. Agronomy, 10(10), Article 10. https://doi.org/10.3390/agronomy10101616

Ruigrok, T., van Henten, E., Booij, J., van Boheemen, K., & Kootstra, G. (2020). Application-specific evaluation of a weed-detection algorithm for plant-specific spraying. Sensors, 20(24), Article 24. https://doi.org/10.3390/s20247262

Shapiro, A., Korkidi, E., Demri, A., Ben-Shahar, O., Riemer, R., & Edan, Y. (2009). Toward elevated agrobotics: Development of a scaled-down prototype for visually guided date palm tree sprayer. Journal of Field Robotics, 26(6–7), 572–590. https://doi.org/10.1002/rob.20299

Spaeth, M., Sökefeld, M., Schwaderer, P., Gauer, M.E., Sturm, D.J., Delatrée, C.C., Gerhards, R., 2024. Smart sprayer a technology for site-specific herbicide application. Crop Protection, 177, 106564. https://doi.org/10.1016/j.cropro.2023.106564

Vijayakumar, V., Ampatzidis, Y., Lacerda, C., Burks, T., Lee, W.S., Schueller, J.K. (2025). AI-driven real-time weed detection and robotic smart spraying for optimized performance and operational speed in vegetable production. Biosystems Engineering, 259, 104288. https://doi.org/10.1016/j.biosystemseng.2025.104288

Vijayakumar, V., Ampatzidis, Y., Schueller, J. K., & Burks, T. (2023). Smart spraying technologies for precision weed management: A review. Smart Agricultural Technology, 6, 100337. https://doi.org/10.1016/j.atech.2023.100337

Vijayakumar, V., Neto, A.D.C., Ampatzidis, Y., Schueller, J.K., Lee, W.S., & Burks, T. (2026). Design and evaluation of a PI-controlled robotic sprayer for precision herbicide applications with multi-nozzle integration. Precision Agriculture, 27, 2. https://doi.org/10.1007/s11119-025-10304-7

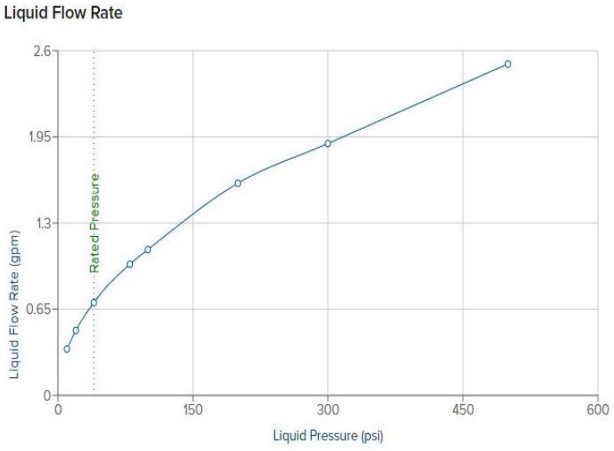
Wolf, R. E., & Bretthaue, S. (2009). Droplet Size Calibration: A New Approach to Effective Spraying. 4.

Wolf, T. (2011), “Sprayer Nozzles”, Agriculture and Agri-Food Canada, Saskatoon.

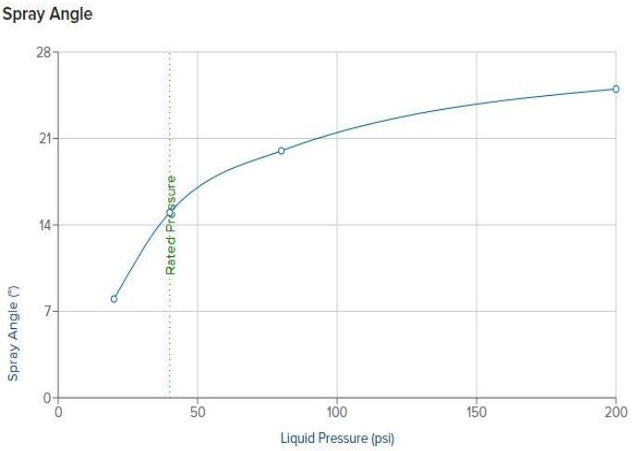
Appendix

Supplementary Table S1. 15° and 25° Veejet nozzle specifications.

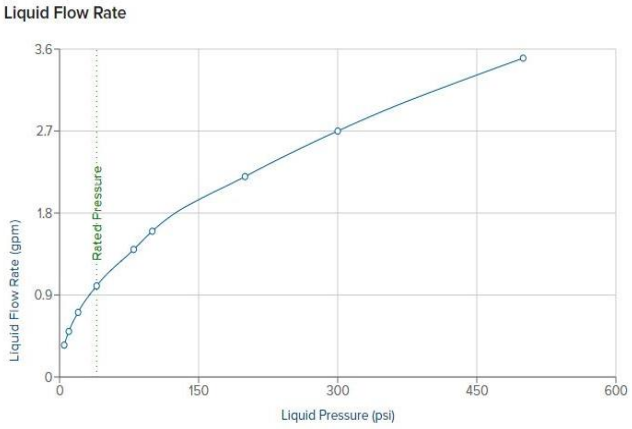
	15° nozzle	**25° nozzle**
Spray pattern	Standard flat-fan tapered edge	Standard flat-fan tapered edge
Spray angle range	8 - 25°	18 - 37°
Spray angle @ pressures	8° @ 137.89 kPa, 15° @ 275.79 kPa	18° @ 137.89 kPa, 25° @ 275.79 kPa
Equivalent orifice diameter	0.167 cm	0.2 cm
Relative drop size range	100 – 500 µm (Light rain), 500 – 1000 µm (Moderate rain)	500 – 1000 µm (Moderate rain), 1000 – 5000 µm (Heavy rain)
Liquid pressure range	68.94 – 3447.38 kPa	34.47 – 3447.38 kPa
Liquid flow rate range	1.33 – 9.47 Lpm	1.33 – 13.26 Lpm



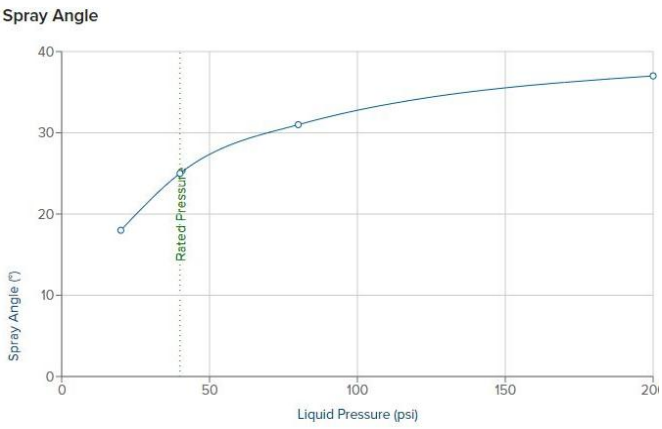
a)



b)



c)



d)

Supplementary Figure S1. Manufacturer-provided performance chart for the 15° and 25° nozzles. The charts show the variation in liquid pressure with liquid flow rate (a and c for the 15° and 25° nozzles, respectively) and with spray angle (b and d for the 15° and 25° nozzles, respectively) (Reference: Spraying Systems Co.).